8-Ali Yılmaz
Field: Atomic and Molecular Physics, Biophysics, NMR Spectroscopy
(Prof.Dr., Batman University, Faculty of Science, Turkey) ali.yimaz@batman.edu.tr
9-Arun Kumar Narayanan Nair
Field: Polymer Chemistry, Computer Simulation
(PhD., King Abdullah University of Science and Technology, Saudi Arabia)
anarayanannair@gmail.com
10-Azeez Abdullah Barzinjy
Field: Material Science, Physics
(Associate Prof.Dr., Materials Science, Department of Physics, Salahaddin University, IRAQ)
azeez.azeez@su.edu.krd
11-Bayram DEMİR
Field: Nuclear Physics, Nuclear Medicine, Medical Imaging
(Prof.Dr., İstanbul University, Faculty of Science, Turkey) bayramdemir69@yahoo.com
12-Birol OTLUDİL
Field: General Biology, Pharmaceutical Biology, Science Education
(Prof.Dr., Dicle University, Faculty of Education, Turkey) birolotludil@dicle.edu.tr
13-Enver SHERIFI
Field: Herbology, Biology, Agricultural Science
(Prof.Dr., University of Prishtina, Kosovo) e_sherifi@yahoo.com
14-Feyyaz DURAP
Field: Inorganic Chemistry
(Prof.Dr., Dicle University, Faculty of Science, Dep. of Chemistry, TURKEY)
fdurap@dicle.edu.tr
15-Gültekin ÖZDEMİR
Field: Agricultural Science, Horticulture
(Prof.Dr., Dicle University, Faculty of Agriculture, Department of Horticulture, Turkey)
gozdemir@gmail.com
16-Hamdi Temel
Field: Pharmaceutical Chemistry
(Prof.Dr., Dicle University, Fac. of Pharmacy, Dep. of Pharmaceutical Chemistry, Turkey)
htemelh@hotmail.com
17-Hasan Çetin ÖZEN
Field: Botany, General Biology
(Prof.Dr., Dicle University, Faculty of Science, Dep. of Biology, Turkey)
hasancetino@gmail.com
18-Hasan İçen
Field: Veterinary Internal Disease
(Prof.Dr., Dicle University, Faculty of Veterinary, Dep. of Internal Disease, TURKEY)
hasanicen@dicle.edu.tr
19-Hasan KÜÇÜKBAY
Field: Organic Chemistry, Peptide Chemistry, Heterocyclic Chemistry, Medicinal Chemistry

(Prof.Dr., İnönü University, Faculty of Science and Letters, Dep. of Chemistry, Turkey)
hkucukbay@gmail.com

20-Hatice Budak GÜMGÜM

Field: Atomic and Molecular Physics, NMR Spectroscopy

(Prof.Dr., Dicle University, Faculty of Science, Dep. of Physics, TURKEY)

hbudakg@gmail.com

21-Hüseyin Alkan

Field: Protein Separation Techniques, Pharmacy

(Assoc.Prof.Dr., Dicle UniversityFaculty of Pharmacy, Department of Biochemistry, TURKEY) mhalkan@dicle.edu.tr

22-Ishtiaq AHMAD

Field: Numerical Analysis, Computer Engineering

(PhD., Austrian Institute of Technology, Austria) ishtiaq.ahmad.fl@ait.ac.at

23-İlhan Dağadur

Field: Mathematics, Analysis and Functions Theory

(Prof.Dr., Mersin University Faculty of Arts and Sciences, Dep. of Mathematics, Turkey) ilhandagdur@yahoo.com; idagadur@mersin@edu.tr

24-İsmail Yener

Field: Analytical Techniques, Pharmacy

(PhD., Dicle University, Faculty of Pharmacy, Department of Analytical Chemistry, Turkey) ismail.yener@dicle.edu.tr

25-Javier FOMBONA

Field: Science Education

(Prof.Dr., University of Oviedo, Spain) fombona@uniovi.es

26-Jonnalagadda Venkateswara Rao

Field: Algebra, General Mathematics

(Prof.Dr., School of Science & Technology, United States International University, Nairobi, KENYA) drjvenkateswararao@gmail.com

27-Lotfi BENSAHLA-TALET

Field: Ecology, Hydrobiology

(Assoc. Prof.Dr.,.Department of Biology, Faculty of Natural Sciences and Life, University Oran1-Ahmed BENBELLA, Algeria) btlotfi1977@gmail.com

28-M.Aydın Ketani

Field: Veterinary, Histology and Embryology

(Prof.Dr., Dicle University, Fac. of Veterinary, Dep. of Histology and Embryology, TURKEY)

29-Mukadder İğdi Şen

Field: Astronautics Engineering

(Dr., Trakya University, Edirne Vocational College of Technical Sciences, Turkey) mukaddersen@trakya.edu.tr

30-Murat Aydemir

Field: Inorganic Chemistry

(Prof.Dr., Dicle University, Faculty of Science, Dep. of Chemistry, TURKEY)
aydemir@dicle.edu.tr

31-Murat Hüdaverdi

Field: High Energy and Plasma Physics

(Dr., Yıldız Technical University, Faculty of Science and Letters, Dep. of Physics, TURKEY)
hudaverd@yildiz.edu.tr

32-Müge Sakar

Field: General Mathematics

(Assoc.Prof.Dr., Dicle University, Turkey) mugesakar@hotmail.com

33-Mustafa AVCI

Field: General Mathematics

(Assoc.Prof.Dr., Batman University, Turkey) mustafa.avci@batman.edu.tr

34-Muzaffer DENLİ

Field: Agricultural Sciences, Animal Science

(Prof.Dr., Dicle University, Faculty of Agriculture, Dep. of Animal Sciences, Turkey)
muzaffer.denli@gmail.com

35-Nuri ÜNAL

Field: High Energy and Plasma Physics

(Retired Prof.Dr., Akdeniz University, Faculty of Science, Turkey) nuriunal@akdeniz.edu.tr

36-Özlem GÜNEY

Field: Mathematics, Analysis and Functions Theory

(Prof.Dr., Dicle University, Faculty of Science, Dep. of Mathematics, Turkey)
ozlemg@dicle.edu.tr

37-Petrica CRISTEA

Field: Computational Physics, Condenced Matter Physics, Electromagnetism

(Assoc.Prof.Dr., University of Bucharest, Faculty of Physics, Romania)
pcristea@fizica.unibuc.ro

38-Sanaa M. Al-Delaimy

Field: Atomic and Molecular Physics, General Physics

(Ph.D., Physics Department, Education College for Pure Sciences, Mosul University, Mosul,
Iraq) sadelaimy@yahoo.com

39-Selahattin Gönen

Field: Physics Education, Science Education

(Prof.Dr., Dicle University, Faculty of Education, Turkey) sgonen@dicle.edu.tr

40-Şemsettin Osmanoğlu

Field: Atomic and Molecular Physics, ESR Spectroscopy

(Prof.Dr., Dicle University, Faculty of Science, Dep. of Physics) sems@dicle.edu.tr

41-Sezai ASUBAY

Field: Solid State Physics

(Prof.Dr., Dicle University, Faculty of Science, Dep. of Physics, Turkey)
sezai.asubay@gmail.com

42-Süleyman DAŞDAĞ

Field: Biophysics

(Prof.Dr., İstanbul Medeniyet University, Faculty of Medicine, Dep. of Biophysics, Turkey) sdasdag@gmail.com

43Yusuf Zeren
Field: Mathematics, Topology
(Assoc.Prof.Dr., Yıldız Technical University, Faculty of Science and Letters, Dep. of Mathematics, TURKEY) yzeren@yildiz.edu.tr

44-Z. Gökay KAYNAK
Field: Nuclear Physics
(Retired Prof.Dr., Uludag University, Faculty of Science, Dep. of Physics, Turkey) kaynak@uludag.edu.tr

CONTENTS

Research Articles

Middle East Journal of Science

Research Article

COMPARATIVE ASSESSMENT OF DOSE CALIBRATORS USED IN NUCLEAR MEDICINE

Merve Cinoğlu Karaca*[1] *Duygu Tuncman Genç [2]* *Hatice Kovan[1]* *Mehmet Mulazımoğlu[1]*
Bayram Demir[2]

[1]Okmeydanı Training and Research Hospital, Department of Nuclear Medicine, Istanbul/TURKEY
[2] Istanbul University, Science Faculty, Physics Department, Istanbul/TURKEY
[*] Corresponding author; mervecinoglu@gmail.com

Abstract: *Dose calibrators are used to measure the amount of radioactive to be given to the patient. It is necessary to determine the correct dose and measure the amount of radioactive material with the least possible error. To minimize these potential errors, quality control (QC) tests should be carried out periodically according to the United States Nuclear Regulatory Authority (NRC). ATOM LAB 400 (serial number:11070208) and 500 (serial number: 15091215) dose calibrators that are actively used in our clinic were used. The aim of this study is to compare with another recently calibrated dose calibrator to verify the dose calibrator that needs to be updated is working properly. QC tests were performed on both dose calibrators. Test results of the currently certified dose calibrator and ATOM LAB 400 dose calibrator whose certificate will be updated were found to be compatible with each other. The tests performed on both dose calibrators remained with the error limits. The calibration certificate of the ATOM LAB 400 calibrator has been updated in accordance with NRC protocol.*
Keywords*: Nuclear Medicine, Dose Calibrator, Quality Control.*

1. Introduction

Nuclear medicine clinics use radiopharmaceuticals with different half-lives for imaging and treatment. These radiopharmaceuticals may be administered to the patient at different activities by means of syringes of different volumes. The radioactive part of the radiopharmaceutical delivered to the patient emits radiation, such as gamma ray or beta particles. Therefore, each activity planned to be given to patients must be measured in a dose calibrator. This activity should be known for the need for radiation protection and successful treatments or good quality imaging [1,2].

Dose calibrators are important in the area of nuclear medicine. Because they are widely used to measure the activity of radioisotopes to be administered to patients. Dose calibrator is a pressurized gas-filled (usually argon gas) cylindrical ionization chamber and it works on the principle of ion chambers. When the radiopharmaceutical to be applied is placed, in the ion chamber, the radiation emitted interacts with the gas in the ion chamber. This interaction results in ion pairs, and when a potential difference is applied between the two electrodes in the ion chamber, the ions travel towards the cathode and the negatively charged ions (electrons) travel towards the anode, hence forming a measurable signal. Then, these signals are converted to current by devices connected to the ion chamber. The total current generated in the ion chamber is directly proportional to the amount of radioactive material. The ion chamber processes the current as a result of the ionization generated by the incoming radiation, allowing

the source activity to be read in Curie (Ci) or Becquerel (Bq) units. Dose calibrator operates over a very wide range of activities, from hundreds of kilobecquerels to tens of Giga Becquerels [3].

The most important part of the dose calibrator is the ionization chamber. The quantity of current produced in the chamber be linked upon the quantity of radioactivity present. Due to distinctness in the types of radiations emitted and photon abundance and energy, equal activities of different radionuclides will generate Technetium-99m (Tc-99m) different current flow [4].

The high-quality isotope calibrators assist responsible staff in nuclear medicine laboratories to perform precise activity measurements and to fulfill the International Commission on Radiological Protection (ICRP) 60 requirement to keep the radiation load as low as achievable for patients. To ensure the measurement accuracy of the dose calibrator, quality control tests must be performed at regular periods. Because routine performance tests are indispensable for evaluating and maintaining equipment efficiency. These tests of the dose calibrator ensure the overall characteristics of the instrument to be within acceptable limits to the user. Accordingly, some standard tests (accuracy, constancy, linearity, geometry, and stability tests) within the aim of these quality control tests are a must. Some of these tests are performed with long half-life standard sources and some with very short half-life isotopes. The accuracy test is carried out using long half-life standard radioisotopes (eg Cesium-137; Cs-137), while the linearity test is performed using short half-life (eg Tc-99m) radioisotopes. Suggested testing procedures and methods of analysis are found in the Nuclear Regulatory Commission Regulatory (NRC) Guide 10. The quality management program enforced by the NRC requires the administration of certain radiopharmaceuticals to be within 5%-10% of the prescribed dose [5,6].

In Turkey, dose calibrators for calibrations are sent to the Turkish Atomic Energy Authority (TAEK) at least once a year. However, during this period, factors such as electricity, humidity, etc. may affect the calibration of the dose calibrator. The one-year calibration period is quite long. Mechanical and electrical damage during this period may affect the dosing calibrator's measuring capacity. This changes the amount of radiation dose to be delivered directly to the patient. In this study, it is aimed to perform the quality control tests of for a dose calibrator by using another newly calibrated calibrator by TAEK. The other objective of this study is to highlight the importance of the quality assurance program in nuclear medicine.

2. Material and Method

ATOM LAB 400 and 500 dose calibrators which are actively used in our clinic were used in this study (Fig.1). We aim to verify the accuracy of the dose calibrator (Atom lab 400) which needs to be updated by using a recently calibrated dose calibrator (Atom lab 500). Accuracy, precision, geometry, and linearity measurement have been performed for two dose calibrators at the Nuclear medicine department, Okmeydanı Training, and Research Hospital, as part of the quality control test. The quality control tests performed on these devices are described below.

Figure 1. Dose calibrators used in this study

2.1. Quality controls of dose calibrators

2.1.1. Physical Inspection

By the time starting the quality control test, the researcher should be checked the instrument housing for evidence of damage. Especially, the researcher should be inspected all controls, check that none are missing, and examine cables, plugs, and sockets for evidence of damage. It should be checked for any accompanying sealed radiation sources for external radioactive contamination.

2.1.2. Geometry Test

Dose calibrator should be provided the same reading for the same amount of activity regardless of the volume or orientation of the sample. This test is designed to show that correct readings can be obtained regardless of the sample size or geometry [7].

First, a reading of a certain amount of Tc-99m activity in a small volume (0,2 cc in our study) is obtained. The volume is then increased by adding the nonradioactive water or saline and additional readings are performed. Each time the liquid increase, the vial is shaken slightly to ensure a homogeneous distribution.

According to NRC limit, the following readings should not vary from the original reading (first reading) by more than 10%. The test is repeated at least once a year [5,6].

2.1.3. Linearity Test (Decaying Source Method)

The linearity test is designed to determine the response of the calibrator over a range of measured activities. A common approach is to use a sample of Tc-99m and sequentially measure it during radioactive decay at its own scale at different times. In the linearity test, the measurement meanwhile calibrator is reported at 6 hours intervals in accordance with the half-life of Tc-99m for a given activity [4].

Background activity is subtracted from the measured value to obtain net activity. In addition, considering the decay law of the radioactive source used, theoretically time-dependent reduction activities are calculated. A comparison is made between the experimental value and the theoretically calculated values.

Due to the fact that the change in activity with time is a definable physical parameter, any deviation in the observed assay value indicates equipment malfunction and nonlinearity. According to NRC, this test is repeated every 15 days. [5,6]

2.1.4. Accuracy and Precision Test

2.1.4.1. Accuracy Test

Accuracy test is a quality control measurement performed upon acceptance, repair, and then annually, to ensure that the activity values determined by the dose calibrator are traceable to standards of radioactivity within the acceptable uncertainties.

The accuracy of the dose calibrator is measured as a part of routine QC of nuclear pharmacy using Cs-137 as a reference source. The background is measure after the source is removed from the dose calibrator. To obtain net activity, we subtract the ground activity from the measured activity. The accuracy test measured 10 times for each device and the results of these measurements are averaged.[8]

The test should be performed at least once a year. Calculations are performed by using the following formula

$$\% \text{ Accuracy} = [(A_{mean} - A_c)/A_c] \times 100$$

In this formula, it means that A_{mean}: mean value of 10 activity measurements,

Ac: The amount of activity on the calibration certificate of the source.

2.1.4.2. Precision Test

The precision test is to confirm that the random uncertainty of a single measurement is primarily determined by the random nature of radioactive decay. It is a measure of the spread of values obtained from a sequence of measurements.

For the precision test, the Cs-137 radioisotope source has 10 measurements on its scale. The background is measured after the sources are removed from the dose calibrator. To obtain net activity, we subtract the ground activity from the measured activity.[8]

Calculations are performed by using the following formula

$$\% \text{ Precision} = [(A_i - A_{mean})/A_{mean}] \times 100$$

A_{mean}: mean value of 10 activity measurements

A_i: Each measured activity value

According to NRC, precision test results should be within $\pm$ 10% error limit. The test should be performed at least once a year[5,6].

2.1.5. Stability and Extended Stability Test

In this test, long half-life Cs-137 radioactive sources are measured using Tc-99m and the other radioisotope scales. To obtain net activity, background activity correction is performed by subtracting the background activity value from the measured activity and these measurements are performed for five days.

According to NRC, The expected result is a maximum deviation of 5% of the measurement results on the other day compared to the first-day measurement. This test should be performed every day. [5,6]

3. Results

3.1. Physical Inspection

No physical damage was detected before the start of quality control tests.

3.2. Geometry Test Result

Geometric deviations may occur as the vial volume expands. This may result in a reduction in the activity measurement of the source. A decrease in the measured activity is an expected situation. However, it should not exceed a ± 5% error. The geometry results are given in Table 1.

Table 1. Geometry test results for both Dose Calibrators

Syringe Volume	Dose Calibrator	
	Atom lab 500 (mCi)	Atom lab 400 (mCi)
0,2 cc *Reference volume*	5,73	5,5
0,3 cc *(Error %)*	5,70 *(-0,52%)*	5,49 *(-0,18%)*
0,5 cc *(Error %)*	5,69 *(-0,69%)*	5,46 *(-0,9%)*
1 cc *(Error %)*	5,64 *(-1,57%)*	5,45 *(-0,9%)*
5 cc *(Error %)*	5,6 *(-2,2%)*	5,37 *(-2,36%)*
10 cc *(Error %)*	5,55 *(-3,14%)*	5,37 *(-2,36%)*
15 cc *(Error %)*	5,55 *(-3,14%)*	5,36 *(-2,54%)*
20 cc *(Error %)*	5,55 *(-3,14%)*	5,6 *(-2,54%)*
25 cc *(Error %)*	5,54 *(-3,13%)*	5,34 *(-2,9%)*
30 cc *(Error %)*	5,53 *(-3,4%)*	5,49 *(-0,18%)*
35 cc *(Error %)*	5,52 *(-3,66%)*	5,33 *(-3,09%)*
40 cc *(Error %)*	5,50 *(-4,0%)*	5,40 *(-1,81%)*
45 cc *(Error %)*	5,49 *(-4,18%)*	5,44 *(-1,09%)*
50 cc *(Error %)*	5,49 *(-4,18%)*	5,42 *(-1,45%)*
55 cc *(Error %)*	5,47 *(-4,5%)*	5,40 *(-1,81%)*
60 cc *(Error %)*	5,45 *(-4,8%)*	5,39 *(-2%)*

mCi: miliCurie

3.3. Linearity (Decaying Source Method) Test Result

Figure 2 shows the theoretically calculated time-dependent reduction of the Tc-99m radioactive source and the activity measurements performed at different hours. When the graph was examined, it was observed that the time-dependent activity decay of the Tc-99m radioactive source was highly consistent with the theoretical calculations.
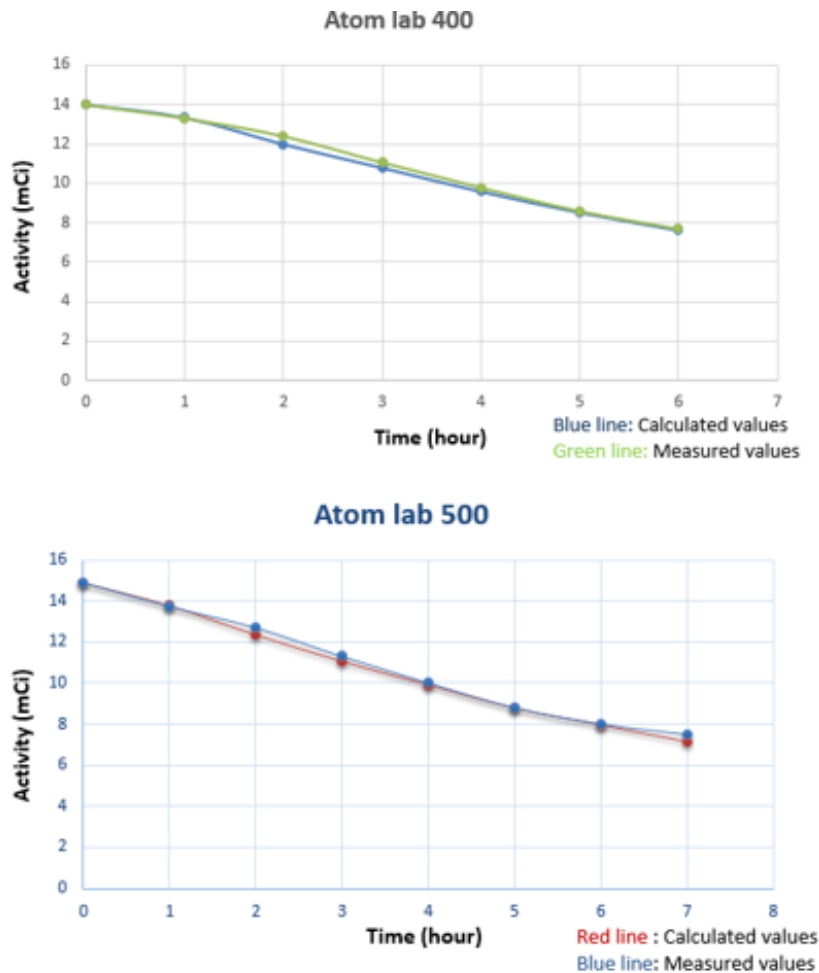
Figure 2. The graphs are drawn using the theoretically calculated values with the radioactive decay formula with measurements performed at every hour for 7 hours.

The reduction of the radioactive material used in the test, calculated according to the radioactive decay theory, is expected to be the same as the reduction of the experimentally measured measurements (Table 2). No value has exceeded the limit.

Table 2. Percentage error limits between measured and calculated activities

Time (hour)	Dose Calibrators	
	Atom lab 500 (% error between measured and calculated activities)	Atom lab 400 (% error between measured and calculated activities)
1st hour	0,3	0,3
2nd hour	3	3
3rd hour	2	2
4th hour	1	2
5th hour	0,07	0,06
6th hour	1	0,09
7th hour	5	5

3.4. Accuracy and Precision Test Results

Accuracy and precision values were calculated with the help of the formulas given in the material and method section. Accuracy results are given in Table 3. And also Precision results are given in Table 4.

Table 3. Accuracy Test Results

	Atom lab 500	Atom lab 400
% Accuracy (Cs-137)	5,5	2,9

Table 4. Precision test results for both Dose Calibrators

PRECISION VALUES – ATOM LAB 500				
Measurement No	Cs-137 Measured Activity (µCİ)	57- Co Measured Activity (µCİ)	Cs-137 Calculated % Precision Values	57-Co Calculated % Precision Values
1	201	239	0	0,42
2	201	238	0	0
3	201	240	0	0,84
4	200	236	-0,49	-0,84
5	201	237	0	-0,42
6	201	238	0	0
7	201	239	0	0,42
8	202	239	0,49	0,42
9	202	236	0,49	-0,84
10	200	238	-0,49	0
Average	201	238		
PRECISION VALUES – ATOM LAB 400				
Measurement No	Cs-137 Measured Activity (µCİ)	57- Co Measured Activity (µCİ)	Cs-137 Calculated % Precision Values	57-Co Calculated % Precision Values

1	195	231	-0,5	0
2	198	231	1,02	0
3	197	232	0,5	0,43
4	197	233	0,5	0,86
5	197	233	0,5	0,86
6	196	226	0	-2,16
7	195	229	-0,5	-0,86
8	197	229	0,5	-0,86
9	195	236	-0,5	-2,16
10	196	231	0	0
Average	196	231		

3.5. Stability and Extended Stability Test Results

Based on the activity value measured in the first day in Table 5, measured in other days activity values are within ± 5% margin of error. Stability and Extended stability results are given in Table 5 for Atom lab 500 Dose Calibrator

Table 5. Five-day activity and ±% error results obtained with Stability and Extended stability test for Atom lab 500 Dose Calibrator.

DAYS ⟍ ISOTOPES	1. DAY Reference Activity	2. DAY	3. DAY	4. DAY	5. DAY
Tc-99m (Error %)	429 µCi	419 µCi (-2,39%)	418 µCi (-2,5%)	420 µCi (-2,09%)	419 µCi (-2,33%)
TI-201 (Error %)	234 µCi	229 µCi (-2,13%)	229 µCi (-2,13%)	229 µCi (-2,13%)	229 µCi (-2,13%)
I-123 (Error %)	152 µCi	149 µCi (-1,97%)	149 µCi (-1,97%)	150 µCi (-1,31%)	149 µCi (-1,97%)
I-131 (Error %)	262 µCi	258 µCi (-1,52%)	257 µCi (-1,9%)	258 µCi (-1,52%)	257 µCi (-1,9%)
Lu-177 (Error %)	1290 µCi	1274 µCi (-0,44%)	1267 µCi (-1,78%)	1270 µCi (-1,55%)	1264 µCi (-2,01%)
Ge/Ga68 (Error %)	113 µCi	111 µCi (-1,76%)	111 µCi (-1,76%)	110 µCi (-2,65%)	110 µCi (-2,65%)

Co-57	391 µCi	385 µCi	384 µCi	380 µCi	380 µCi
(Error %)		*(-1,53%)*	*(-1,79%)*	*(-2,81%)*	*(-2,81%)*
Ga-67	363 µCi	358 µCi	356 µCi	357 µCi	355 µCi
(Error %)		*(-1,37%)*	*(-1,92%)*	*(-1,92%)*	*(-2,20%)*
In-111	146 µCi	144 µCi	144 µCi	143 µCi	143 µCi
(Error %)		*(-1,36%)*	*(-1,36%)*	*(-2,05%)*	*(-2,05%)*
F-18	107 µCi	106 µCi	105 µCi	105 µCi	105 µCi
(Error %)		*(-0,93%)*	*(-1,86%)*	*(-1,86%)*	*(-1,86%)*
Y-90s	3,91 µCi	3,86 µCi	3,82 µCi	3,80 µCi	3,8 µCi
(Error %)		*(-1,27%)*	*(-2,30%)*	*(-2,82%)*	*(-2,82%)*
Cs-137	201 µCi	199 µCi	197 µCi	197 µCi	197 µCi
(Error %)		*(-0,99%)*	*(-1,97%)*	*(-1,97%)*	*(-1,97%)*
Ba-133	82 µCi	81 µCi	81 µCi	80 µCi	80 µCi
(Error %)		*(-1,21%)*	*(-1,21%)*	*(-2,43%)*	*(-2,43%)*
Mo-99	1954 µCi	1927 µCi	1914 µCi	1927 µCi	1917 µCi
(Error %)		*(-1,38%)*	*(-2,04%)*	*(-1,38%)*	*(-2,04%)*
Sr-89	7,66 µCi	7,54 µCi	7,5 µCi	7,5 µCi	7,5 µCi
(Error %)		*(-1,59%)*	*(-2,08%)*	*(-2,08%)*	*(-2,08%)*

Stability and Extended stability results are given in Table 6 for Atom lab 400 Dose Calibrator.

Table 6. Five-day activity and ±% error results obtained with Stability and Extended stability test for Atom lab 400 Dose Calibrator.

DAYS / ISOTOPES	1.DAY *Reference Activities*	2. DAY	3. DAY	4. DAY	5. DAY
Tc-99m	405 µCi	418 µCi	420 µCi	418 µCi	418 µCi
(Error %)		*(2,20%)*	*(3,7%)*	*(1,7%)*	*(1,7%)*
TI-201	235 µCi	237 µCi	236 µCi	235 µCi	235 µCi
(Error %)		*(0,85%)*	*(0,43%)*	*(0%)*	*(0%)*
I-123	144 µCi	145 µCi	144 µCi	144 µCi	144 µCi
(Error %)		*(0,69%)*	*(0%)*	*(0%)*	*(0%)*
I-131	242 µCi	252 µCi	251 µCi	251 µCi	251 µCi
(Error %)		*(4,13%)*	*(3,72%)*	*(3,72%)*	*(3,72%)*

Lu-177	1278 µCi	1287 µCi	1286 µCi	1285 µCi	1279 µCi
(Error %)		*(0,7%)*	*(0,62%)*	*(0,54%)*	*(0,07%)*
Ge/Ga68	113 µCi	114 µCi	114 µCi	114 µCi	113 µCi
(Error %)		*(0,88%)*	*(0,88%)*	*(0,88%)*	*(0%)*
Co-57	364 µCi	382 µCi	380 µCi	380 µCi	379 µCi
(Error %)		*(4,9%)*	*(4,39%)*	*(4,39%)*	*(4,12%)*
Ga-67	364 µCi	367 µCi	367 µCi	366 µCi	354 µCi
(Error %)		*(0,82%)*	*(0,82%)*	*(0,54%)*	*(-2,74%)*
In-111	140 µCi	146 µCi	146 µCi	146 µCi	146 µCi
(Error %)		*(4,28%)*	*(4,28%)*	*(4,28%)*	*(4,28%)*
F-18	107 µCi	108 µCi	108 µCi	108 µCi	108 µCi
(Error %)		*(0,93%)*	*(0,93%)*	*(0,93%)*	*(0,93%)*
Y-90s	3,92 µCi	3,9 µCi	3,94 µCi	3,94 µCi	3,93 µCi
(Error %)		*(-0,51%)*	*(0,50%)*	*(0,50%)*	*(0,25%)*
Cs-137	191 µCi	194 µCi	193 µCi	193 µCi	192 µCi
(Error %)		*(1,57%)*	*(1,04%)*	*(1,04%)*	*(0,52%)*
Ba-133	83 µCi	84 µCi	83 µCi	83 µCi	83 µCi
(Error %)		*(1,20%)*	*(1,21%)*	*(0%)*	*(0%)*
Mo-99	1964 µCi	1978 µCi	1969 µCi	1969 µCi	1964 µCi
(Error %)		*(0,72%)*	*(0,25%)*	*(0,25%)*	*(0%)*
Sr-89	7,69 µCi	7,75 µCi	7,71 µCi	7,71 µCi	7,7 µCi
(Error %)		*(0,78%)*	*(0,26%)*	*(0,26%)*	*(0,13%)*

4. Discussion

The main objective in nuclear medicine applications is to get the best image with minimum and accurately measured radiation. The availability of dose calibrators and regular quality control tests in nuclear medicine centers is one of the requirements of IAEA for the determination of these dosage amounts given to the patient in the most efficient way. Optimization refers to the principle that the radiation dose to the patients should be "as low as reasonably achievable (ALARA)". The main efforts for optimization of radiation protection in nuclear medicine have been made in terms of the reduction of administered radiopharmaceutical activity [9]. The ALARA principle is important for patients as well as workers.

Our clinic is conducted with two different radioisotope calibrators branded Biodex ATOM LAB-500 and Biodex ATOM LAB 400. The quality controls of the devices are extremely important in terms of giving the patient minimum radiation. Even though very small doses are administered to the patient in nuclear medicine applications, these small doses should also be completely accurate, especially for a child patient. For this; the fact that the factory settings of an electronic system can change continuously, the right tests at the right times are essential for patient health and success in the examination. This study was carried out in a nuclear medicine center with high patient capacity. Test results of the currently certified dose calibrator and ATOM LAB 400 dose calibrator which hasn't got certificate updated were found to be compatible with each other. The tests performed on both dose

calibrators remained with the error limits. The calibration certificate of the ATOM LAB 400 calibrator has been updated in accordance with NRC protocol in our department.

In our study, for the Geometry test, the doses of the calibrators decreases as the radioactive material in the syringe moves away from the center (Table 1). When the error value of the measured values is examined according to the measurement results from 0,2 cc, it is seen that the deviation occurred within ± 5% error.

For the linearity test, it is observed that the time-dependent activity reduction of the Tc-99m radioactive source is quite consistent with the theoretical calculations for two-dose calibrators (Figure 2).

In our study, Tc-99m, which has a half-life of 6 hours, was used in the test of linearity. As shown in Table 2, the calculated error increases after the sixth hour. The error results from both calibrators were similar.

In the study of Koç, the measurement for linearity tests were performed with two different radioisotope calibrators, Capintec 15R and Biodex ATOM LAB 500 in a Nuclear Medicine Center. These measurements, linearity tests of devices have been performed by using the method of decaying source, increasing source, and sample -volume effect [10].

In the study of Koç, the results show that both calibrators have a very high performance, but the first calibrator (Capintec 15 R) has about 1% better performance. The results of the method used for the linearity test in our study and the decaying source method used by Koç in their study are consistent with each other.

In our study, accuracy values were calculated for Cs-137according to the accuracy formula. 5.5 % accuracy value was calculated for Atom lab 500 and 2.9 % accuracy value was calculated for Atom lab 400 (Table 3).

The precision of a measurement is determined by how close it is to the true value (reference condition) [11]. When % precision values are examined for both dose calibrators, it is seen that calculated % accuracy values are within the 5% limit (Table 4).

In Table 5 and Table 6, the activity values measured on the other days are within ± 5% error according to the activity value observed on the first day. For the Stability and Extended Stability test in Table 6 and Table 7, it is seen that the margins of error are very small and dose calibrators perform very stable repetitions.

In Mohamed's study, four different quality control tests were performed using two standard radionuclides, Cs-137, and Co-57, which are accuracy, stability, linearity, and geometry for two-dose calibrators in different medical departments. [11]. All results obtained from the study have been compared with the international standard (±5%) and the results showed that two-dose calibrators have good performance and there is no need for any correction tables or factors or maintenance. In Muhammed's study, the results of accuracy showed that two-dose calibrators have accurate reading and the percentage of error was 0.39% which was accepted. The percentage of accuracy of dose calibrator was easily detected by using the accuracy equation. Quality control test results of Mohammed's study are consistent with our study.

In the Alameen study, four quality-control tests accuracy, constancy, linearity, and geometry tests were performed for two-dose calibrators, Capintec PTW CURIEMENTOR4, and Capintec CRC-25R. The results of quality control tests revealed that the parameters monitored for dose calibrators were within the limits of international standards. (±5%) [12].

As a result of the measurements made for our quality control tests, it was found that the performances of both calibrators (Atom lab 400 and Atom lab 500) in the clinic were within the determined limits and were quite good. It is thought that the reason for the high performance of the devices is the continuous quality control studies.

5. Conclusions

According to the current standards and regulations for Nuclear Medicine worldwide practices, the radioactivity of any radiopharmaceutical that contains a photon emitting radionuclide must be measured by a dose calibrator prior to administration to patients or for human research purposes [9]. The calibration period of one year is quite long for these devices. Mechanical and electrical damage during this time may affect the dosing calibrator's measuring capacity. Any damage such as electrical fault may change the amount of radiation dose to deliver directly to the patient. We have repeated the tests of a calibrator exposed to electrical damage in accordance with such a situation by using a current calibrated dose certificate for another dose calibrator.

The compliance to the Research and Publication Ethics: This study was carried out in accordance with the rules of research and publication ethics.

References

[1] Demir, B., Kaplan, A. et al., "Production cross-section calculations of medical 32p, 117sn, 153sm And 186,188re radionuclides used In Bone Pain Palliation Treatment", *KERNTECHNIK*, 80, 58-65, 2015.

[2]Alameen, S., Bdelfatah, AM. et.al., "Assessment of Dose Calibrators Performance in Nuclear Medicine Department in Sudan", *Sch. Acad. J. Pharm.*, 5, 245-250, 2016.

[3]Dale, JW., "A beta-gamma ionization chamber for substandards of radioactivity-11. Instrument response to gamma radiation", *Int J Appl Radiat.*, 10, 72-78, 1961.

[4]Kowalsky, RJ., Jonston, RE. et al., "Dose Calibrator Performance and Quality Control", *J. Nucl. Med. Technol.*, 5, 35-40, 1977.

[5] Tunçman Genç, D., Poyraz L., et al., "Nükleer tıpta kullanılan doz kalibratörlerinin kalite control testleri", *FNG &Demiroğlu Bilim Tıp Dergisi*, 5, 8-14, 2019.

[6] U.S. Nuclear Regulatory Commission Code of Federal Regulations. Title 10, Part 35, Washington D.C., April 1987, Updated January 24, 2018.

[7]Zanzonico, P., "Routine quality control of clinical nuclear medicine instrumentation: a brief review", *J Nucl Med,*49, 1114-31, 2008.

[8]Özkırlı, M., Bor, D.et al., "Dozkalibratörlerininperformansözelliklerininkıyaslanması", *TJNM*, 4, 143-8, 1995.

[9] Cho, SG., Kim, J., et al., "Radiation Safety in Nuclear Medicine Procedures", *Nucl Med Mol Imaging*, 51, 11–16, 2017.

[10]Koç, K.,"Nükleer Tıp merkezlerinde kullanılan radyoizotop kalibratörlerinde kalite sağlanması üzerine bir araştırma-lineerite testi", *Politeknik*; 21, 507-11, 2018.

[11] Aya, Mohammed., Mudthir MHO. et al., "Assessment of Tc-99m Dose Calibrator Performance in Nuclear Medicine Department", *International Journal of Science and Research (IJSR)*. 11,36-39,2014.

[12] Alameen, S., Bdelfatah, AM. et al., "Assessment of Dose Calibrators Performance in Nuclear Medicine Department in Sudan", *Sch. Acad. J. Pharm.*, 5, 245-250, 2016.

Middle East Journal of Science

Research Article

EVALUATION OF PHYTOCHEMICAL CONSTITUENTS IN THE WHOLE PLANT PARTS OF HEXANE EXTRACT OF SOME TRADITIONAL MEDICINAL PLANTS BY GC-MS ANALYSIS

Alevcan KAPLAN[1]* ⓘ   *Umut ÇELİKOĞLU[2]* ⓘ

[1]Sason Vocational School, Department of Crop and Animal Production, Batman University, 72060 Batman, Turkey
[2]Department of Chemistry, Faculty of Arts & Science, Amasya University, 05100, Amasya, Turkey- Orcid No:
*Corresponding author:kaplanalevcan@gmail.com

Abstract: *The aim of this study was to determine the phytochemical components from the hexane extract of some medicinal plants (Salvia palaestina Bentham, Alkanna trichophila var. mardinensis Hub-Mor. (an endemic* variety*), Scutellaria orientalis L. and to evaluate its biological activity by GC-MS analysis. The chemical components in this hexane extract were subjected to the Agilent 7890B GC-5977MSD model Gas Chromatography - Mass Spectrometric analysis. Thirty-two chemical compounds have been identified in the plant extracts. This definition is based on the peak area, retention time, molecular weight, and molecular formula. In this research, Bis (2-ethylhexyl) phthalate, tricosane, docosane, transcaryophyllene, nonacosane, beta-Cubebene, Trichlorfon, Naphthalene, 1,2,3,4,4a, 5,6,8a-octahydro-4a, 8-dimethyl -2- (1-methylet henyl) -, [2R, 3-Aminophenol were found predominantly compounds in extracts. These compounds, which we identified in our study, have a wide range of biological activity and have been found to have high therapeutic value. They are candidate plants to be medicines with various active ingredient content.*

Keywords: *GC-MS analysis, medicinal plants, phytochemical constituents, therapeutic*

1.Introduction

Turkey is among the richest countries in the world in terms of plant diversity. Although it is about 15 times smaller than Europe in terms of surface area, it has plant diversity as much as European continental flora in terms of flora. The main reasons for this wealth are as follow; a variety of climates, topographical diversity with marked changes in ecological factors over short distance, geological and geomorphic variation, a range of aquatic environments such as seas, lakes, and rivers, altitude variations from sea level to 5000 [1]. The total number of species and subspecies taxa in our country is 11 707 including the foreign origin and cultivated plants [2]. It is estimated that the type of plants used for medicinal purposes is around 1000 [3]. Medicinal plants are part of the nature pharmacy. Despite important advances in medicine, people have sought healing from time to time and have never stopped using medicinal plants as a result of their experience for centuries. Especially the emergence of side effects of synthetic and chemical drugs has increased the use of medicinal plants. Medicinal plants spice, pharmaceutical industry, soft drink, perfume, soap, confectionery, cosmetics, toothpaste, chewing

gum, healing and relaxing tea manufacture, essential oil, aroma, etc. it is used in many fields [4]. In addition, natural products, pure compounds or standard herbal extracts offer unlimited opportunities to obtain new medicines due to the unique availability of chemical diversity. The knowledge gained about the chemical constituents of plants will be more useful in discovering the true value of folk remedies [5].

In the present study, it was aimed to determine the preliminary phytochemical analysis of *Salvia palaestina* Bentham, *Alkanna trichophila* var. *mardinensis* Hub.-Mor. (an endemic variety), *Scutellaria orientalis* L. which has not been studied before, which grows in the untouched Mount Raman, Batman. For this reason, phytochemical screening of the species in question during current research is carried out in order to analyze the presence of chemical compounds, which are secondary metabolites, in order to suggest their application in the pharmaceutical industry.

2. Materials and Methods
2.1. Collection and identification of plant samples

The plant samples were collected from the natural habitat of the Batı Raman campus in Batman University. Voucher specimens have been deposited at the Batman University (voucher no. 2020/015, 2020/016, and 2020/014, respectively) (Figure 1). The taxonomical identity of the plant was confirmed by Dr. Alevcan Kaplan. This identification was made using, Flora of Turkey, Volume 6-7. [6,7]. The collected, whole parts of plants were washed to remove dust and other plant materials and were shade dried at room temperature. The dried leaves and flowers were then ground to a powder using an electric grinder and kept separately for future research in lidded containers.
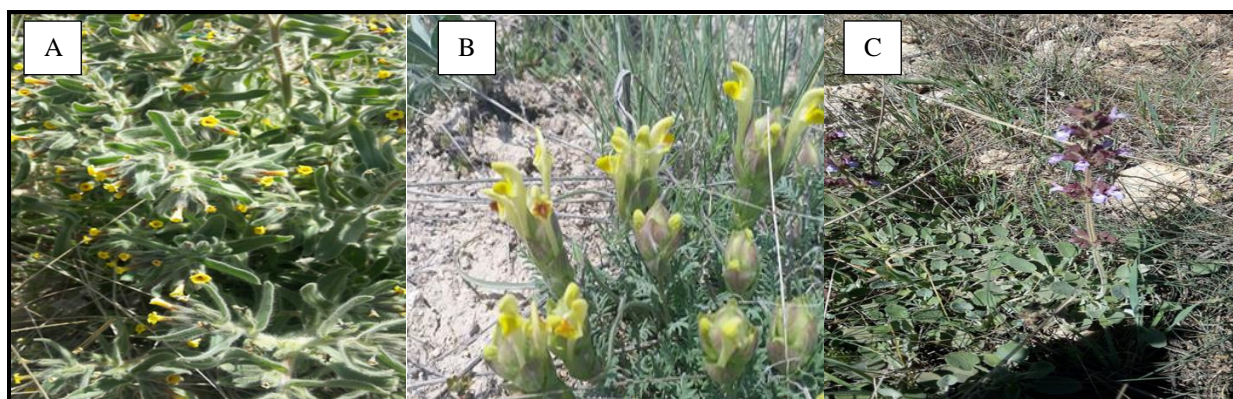
Figure 1. General view of plants (A: *Alkanna trichophila* var. *mardinensis* B: *Scutellaria orientalis* C: *Salvia palaestina*) Photo: A. Kaplan

2.2. Plant Sample Preparation for GC-MS

The n-hexane extract of the plants was obtained using the Soxhlet extractor. 10 g of powdered plant samples were put into the Soxhlet extractor and the required amount was obtained by repeatedly using 100 ml of n-hexane (boiling point about 40 - 60 °C) as solvent extract for four (4) hours. The oil was kept in a refrigerator without further processing until required for analysis.

2.3. GC-MS Data Analysis Condition

Gas chromatography-Mass spectrometry (GC-MS) analysis of n-hexane extracts of plants was performed using Agilent 7890B GC- 5977MSD model with the column length (30 m), diameter (250

μm), and film thickness (0.25 μm) was used with Helium (99.9995 % purity) as the carrier gas, operating in electron impact mode at 70 eV. and the GS-MS condition during the research is following conditions. Injector temperature was 250 ℃, ion-source temperature 200 ℃ split flow was 2.4 ml/min. The oven temperature was programmed 120 ℃ (5 ℃ / min, 7 min), 150 ℃ (5 ℃ / min, 7 min), 200 ℃ (5 ℃ / min, 7 min), 220 ℃ (5 ℃ / min, 7 min), 240 ℃ (5 ℃ / min, 7 min), 250 ℃ (5 ℃ / min, 7 min). The split flow was 2.4 ml/min and an injection volume of 1 μ1 was employed (split ratio of 2:1). The hexane extract of plants was injected with syringe manually for total bioactive components of leaf and flower samples. Total GC running time is 68 min.

2.4. Identification of constituents

The identity of the constituents in the extract is assigned by comparison of retention times and mass spectra with those stored in the computer fragmentation models library and also with electronic libraries (W9N11.L, MPW2011.L and RTLPEST3.L). Electronic Libraries sources were also used to match the components identified from the plant material. The name, the nature of the compound, molecular weight, molecular formula of the components of the test materials have been confirmed.

3. Results and Discussion

Traditional medicine and food in many plants used Turkey is one of the world's richest countries in terms of genetic diversity. The main reasons for the richness of plant species in Turkey are different climates and soil types and topography as a result of other environmental conditions. In Anatolia folk medicine, medicinal plants have an important place in the field of health both in the world and in our country. Therefore, it is important to conduct research on such plants containing a variety of phytochemicals as it has a high potential to result in cost-effective drug intervention with fewer side effects.

In this study, phytochemical constituents of *Alkanna trichophila* var. *mardinensis*, *Scutellaria orientalis* and *Salvia palaestina* were identified and characterized respectively. In this respect, nine compounds were identified in *Alkanna trichophila* var. *mardinensis* by GC-MS analysis (Table 1). The list of phytochemical compounds from the plant sample is tabulated in Table 1 with retention time, area, and area percentage. The chromatogram information for the sample is given in Figure 2. The retention time taken by the bioactive compounds of the plant sample varied from 31.183 to 65.168. It was found that main constituents of sample were 13-Octadecenal (1.84 %), Tetradecanal (0.65 %), Dinocap II (3.32 %), Bis(2-ethylhexyl) pht-halate (60.60 %), alpha-Amyrin (3.43 %), Metolcarb (1.58 %), Tricosane (12.44 %), Octacosane (7.50 %), Docosane (8.64 %). The compound phenol 13-Octadecenal is known for its sex pheromone, antimicrobial activity [8,9]. Tetradecanal is known for immunotoxicity activity. bacterial bioluminescence, sex pheromone *Heliothis virescens* (F.) females [10, 11, 12]. Dinocap II has been reported to contact fungicide used to control powdery mildew on many crops and is also used as a non-systemic acaricide [13]. Bis (2-ethylhexyl) pht-halate has a role as an apoptosis inhibitor, an androstane receptor agonist and a plasticiser. Moreover, it has an anti-leukaemic, anti-mutagenic, antimicrobial, and cytotoxic activity [14,15]. Alpha-Amyrin is known for attenuates orofacial pain, reducing hyperalgesia, anti-inflammatory effects [16,17]. Metolcarb is an insecticide [18]. Tricosane has been reported to bear antimicrobial activity and influence host egg parasitisation by Trichogramma [19,20]. Octacosane is known to possess antimicrobial, antioxidant, and anti-inflammatory [21,22]. Docosane is reported to aid in host egg parasitization that can be used as a bio-control agent, antimicrobial, antioxidant, and functional food nutraceutical applications [23,24,25]. In

light of this information, it has been determined that the plant constituting our experimental material contains different amounts of bioactive components with various therapeutic effects. The potential of the plant to be used in the treatment of diseases such as antileukemia, which is the most common disease of today, has been revealed, especially due to its high content of Bis (2-ethylhexyl) pht-halate. [15] reported that Bis (2-ethylhexyl) pht-halate isolated from *Aloe vera* L. showed anti-leukemic and anti-mutagenic effects (*Salmonella typhimurium* TA98 and TA100 strains). [26] found that di- (2-ethylhexyl) phthalate (DEHP) isolated from *Calotropis gigantea* L. flowers had an antitumor effect. We determined that our plant in question has a feature that can be used in the treatment of these diseases.

Table 1. Phytochemical constituents of *Alkanna trichophila* var. *mardinensis* by GC-MS

No	Name of the compound	Molecular formula	Molecular weight	RT	Peak area(%)	Nature of the compound
1	13-Octadecenal,	$C_{18}H_{34}O$	266.5 g/mol	31.183	1.84	-
2	Tetradecanal,	$C_{14}H_{28}O$	212.37 g/mol	31.884	0.65	fatty aldehyde
3	Dinocap II,	$C_{18}H_{24}N_2O_6$	364.39 g/mol	42.215	3.32	enoate ester
4	Bis(2-ethylhexyl) phthalate,	$C_{24}H_{38}O_4$	390.6 g/mol	50.157	60.60	phthalate ester
5	alpha-Amyrin,	$C_{30}H_{50}O$	426.7 g/mol	53.434	3.43	pentacyclic triterpenoid
6	Metolcarb	$C_9H_{11}NO_2$	165.19 g/mol	54.608	1.58	carbamate ester
7	Tricosane	$C_{23}H_{48}$	324.6 g/mol	56.754	12.44	N-Alkanes
8	Octacosane	$C_{28}H_{58}$	394.8 g/mol	57.055	7.50	N-Alkanes
9	Docosane	$C_{22}H_{46}$	310.6 g/mol	65.168	8.64	N-Alkanes
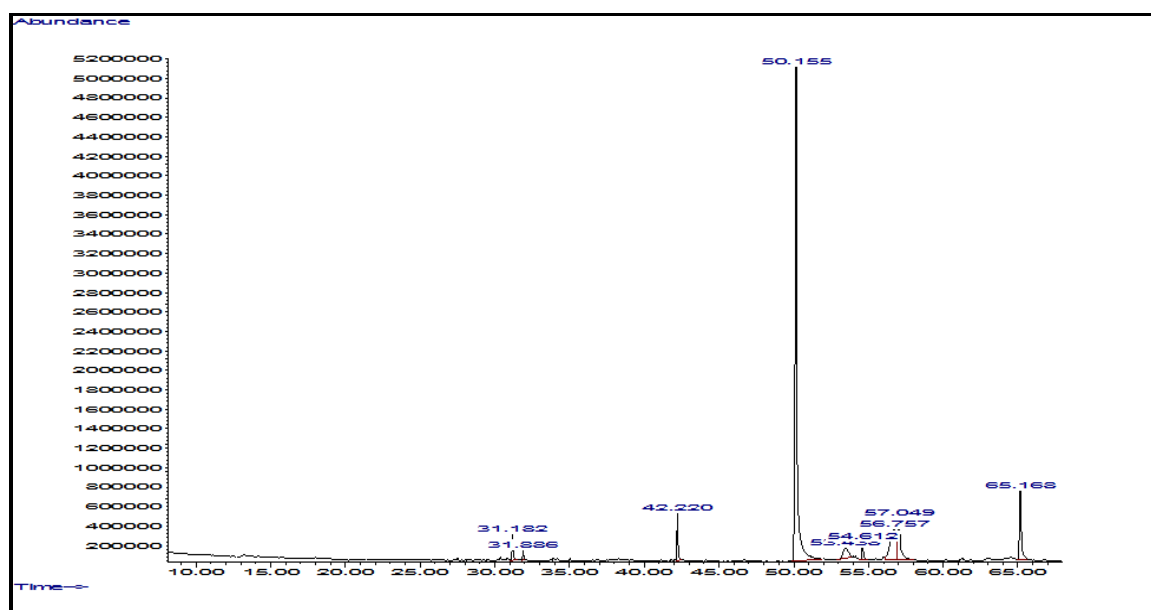
Figure 2. GC- MS chromatogram of the hexane fraction of compounds from *Alkanna trichophila* var. *mardinensis*

Secondly, eleven compounds were identified in *Scutellaria orientalis* by GC-MS analysis (Table 2). The list of phytochemical compounds from the plant sample is tabulated in Table 2 with retention time, area, and area percentage. The chromatogram information for the sample is given in Figure 3. The retention time taken by the bioactive compounds of the plant sample varied from 0.93 to 28.83. It was found that main constituents of sample were 2-Ethyl-1,3-hexanediol (2.97 %), Tryclopyrbutoxy-ethyl (1.66 %), trans-Caryophyllene (28.83 %), beta-Cubebene (6.46 %), Tris(2-butoxyethyl) phosphate (0.93 %), Diisobutyl phthalate (0.65 %), Eicosane (2.44 %), 1-Triacontanol (3.48 %), Heptaco-

sane (5.19 %), 1-Heptacosanol (5.13 %), Nonacosane (16.14 %). 2-Ethyl-1,3-hexanediol has an antiparasitic, insecticidal, and repellent, ectoparasiticidal effect [27]. Tryclopyrbutoxyethyl is known to pesticide [28]. Trans-caryophyllene is also known as antibacterial and antifungal [29]. Beta-Cubebene has been reported that neuroprotective effects [30]. Tris (2-butoxyethyl) phosphate (TBEOP) is an organophosphate [31]. Diisobutyl phthalate also known proliferation and differentiation of primary osteoblasts, antioxidant, and free radical scavenging activities [32,33]. Eicosane has been reported that an antitumor activity [34]. 1-Triacontanol (TRIA) is a growth regulator for plants [35]. Heptacosane has shown antioxidant, antibacterial, antimalarial, antidermatophytic effects [36,37,38]. 1-Heptacosanol is known for its antimicrobial activity [39]. Nonacosane has also known as celidoniol deoxy antibacterial and anti-inflammatory [40,41]. It is clear that the plant in question contains bioactive components with broader effects. Our study results support the potential of the plant to be used ethnobotanically in the region.

Table 2. Phytochemical constituents of *Scutellaria orientalis* by GC-MS

| No	Name of the compound	Molecular formula	Molecular weight	RT	Peak area (%)	Nature of the compound
1	2-Ethyl-1,3-hexanediol	$C_8H_{18}O_2$	146.23 g/mol	9.160	2.97	Aliphatic alcohol
2	Tryclopyrbutoxyethyl	$C_{13}H_{16}Cl_3NO_4$	356.6 g/mol	10.405	1.66	-
3	trans-Caryophyllene	$C_{15}H_{24}$	204.35 g/mol	11.607	28.83	Bicyclic sesquiterpene
4	beta-Cubebene	$C_{15}H_{24}$	204.35 g/mol	11.879	6.46	Tricyclic sesquiterpene
5	Tris(2-butoxyethyl) phosphate	$C_{18}H_{39}O_7P$	398.5 g/mol	14.469	0.93	-
6	Diisobutyl phthalate	$C_{16}H_{22}O_4$	278.34 g/mol	27.062	0.65	Phthalate ester
7	Eicosane	$C_{20}H_{42}$	282.5 g/mol	50.143	2.44	N-Alkanes
8	1-Triacontanol	$C_{30}H_{62}O$	438.8 g/mol	56.010	3.48	Fatty alcohol
9	Heptacosane	$C_{27}H_{56}$	380.7 g/mol	57.055	5.19	N-Alkanes
10	1-Heptacosanol	$C_{27}H_{56}O$	396.7 g/mol	64.152	5.13	Fatty alcohol
11	Nonacosane	$C_{29}H_{60}$	408.8 g/mol	65.154	16.14	N-Alkanes
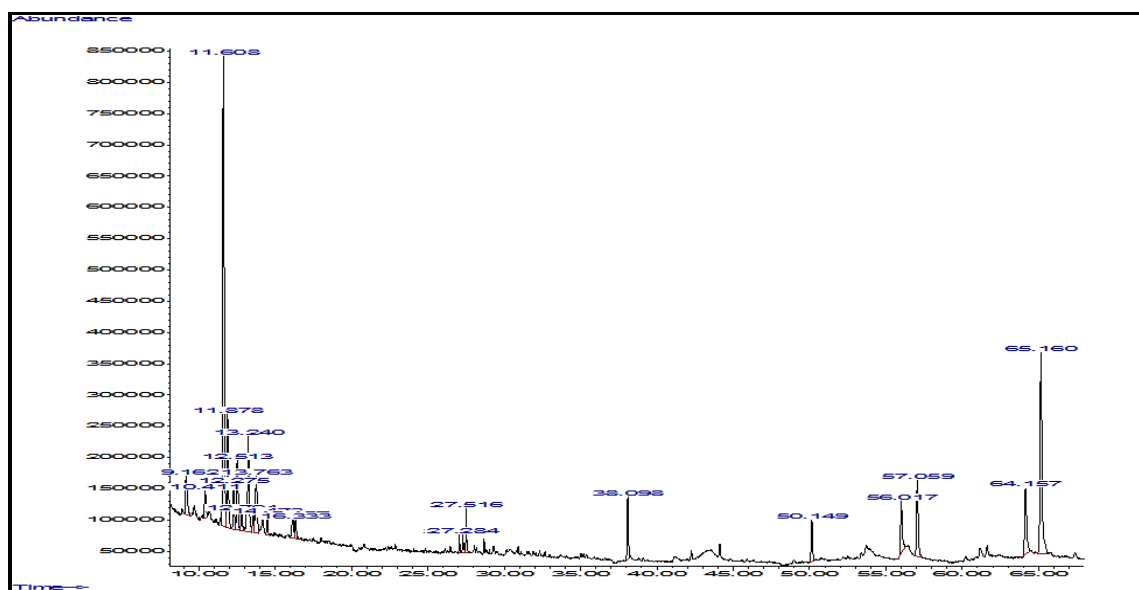
Figure 3. GC- MS chromatogram of the hexane fraction of compounds from *Scutellaria Orientalis*

Thirdly, twelve compounds were identified in *Salvia palaestina* by GC-MS analysis (Table 3). The list of phytochemical compounds from the plant sample is tabulated in Table 3 with retention

time, area, and area percentage. The chromatogram information for the sample is given in Figure 4. The retention time taken by the bioactive compounds of the plant sample varied from 0.22 to 79.15. It was found that main constituents of sample were trans-Caryophyllene (1.43 %), Neophytadiene (0.22 %), Sclareoloxide (0.61 %), geranyl-p-cymene (0.22 %), Caryophyllene (0.96 %), 3-Aminophenol (1.47 %), Trichlorfon (79.15 %), Naphthalene, 1,2,3,4,4a,5,6,8a-octahydro-4a,8-dimethyl-2-(1-methylet henyl)-, [2R (5.84%), Allidochlor (0.25 %), Isobornyl thiocyanoacetate (1.03 %), Heptacosane (0.64 %), Nonacosane (0.71 %). Neophytadiene is an antipyretic, analgesic, anti-inflammatory, anti-microbial, antioxidant [42]. Sclareoloxide is known to demonstrate good antimicrobial activity, antioxidant and antiviral activities [43]. Geranyl-p-cymene has been reported that an antimicrobial, antioxidant, and antiproliferative effect [44]. Caryophyllene is also known as anticancer, antioxidant, and antimicrobial [45]. 3-Aminophenol is an antibacterial [46]. Trichlorfon is known for its insecticidal effects [47]. Naphthalene, 1,2,3,4,4a,5,6,8a-octahydro-4a,8-dimethyl-2-(1-methylet henyl)-, [2R is an insecticide, repellant [48]. Allidochlor is the more active herbicide and has been introduced into agricultural use [49]. Isobornyl thiocyanoacetate is an insecticide and used to control ants, houseflies, and head lice [50]. In this study, it was clearly demonstrated that Salvia palaestina has the potential to be used as an insecticidal because of the high rate of triclorfon in addition to the various therapeutic substances it contains.

Table 3. Phytochemical constituents of *Salvia palaestina* by GC-MS

No	Name of the compound	Molecular formula	Molecular weight	RT	Peak area(%)	Nature of the compound
1	trans-Caryophyllene	$C_{15}H_{24}$	204.35g/mol	11.607	1.43	Bicyclic sesquiterpene
2	Neophytadiene	$C_{20}H_{38}$	278.5 g/mol	27.519	0.22	Terpenes
3	Sclareoloxide	$C_{18}H_{30}O$	262.4 g/mol	28.049	0.61	Diterpene
4	geranyl-p-cymene	$C_{18}H_{26}$	242.4 g/mol	30.081	0.22	Homoditerpenes
5	Caryophyllene	$C_{15}H_{24}$	204.35 g/mol	32.986	0.96	Bicyclic sesquiterpene
6	3-Aminophenol	C_6H_7NO	109.13 g/mol	33.701	1.47	Aminophenol
7	Trichlorfon	$C_4H_8Cl_3O_4P$	257.43 g/mol	38.481	79.15	Phosphonic ester
8	Naphthalene, 1,2,3,4,4a,5,6,8a-octahydro-4a,8-dimethyl-2-(1-methylet henyl)-, [2R	$C_{15}H_{24}$	204.3511 g/mol	39.311	5.84	Polycyclic hydrocarbon
9	Allidochlor	$C_8H_{12}ClNO$	173.64 g/mol	39.525	0.25	Carboxamide
10	Isobornyl thiocyanoace-tate	$C_{13}H_{19}NO_2S$	253.36 g/mol	44.333	1.03	Thiocyanoacetic acid ester
11	Heptacosane	$C_{27}H_{56}$	380.7 g/mol	57.069	0.64	N-Alkanes
12	Nonacosane	$C_{29}H_{60}$	408.8 g/mol	65.168	0.71	N-Alkanes
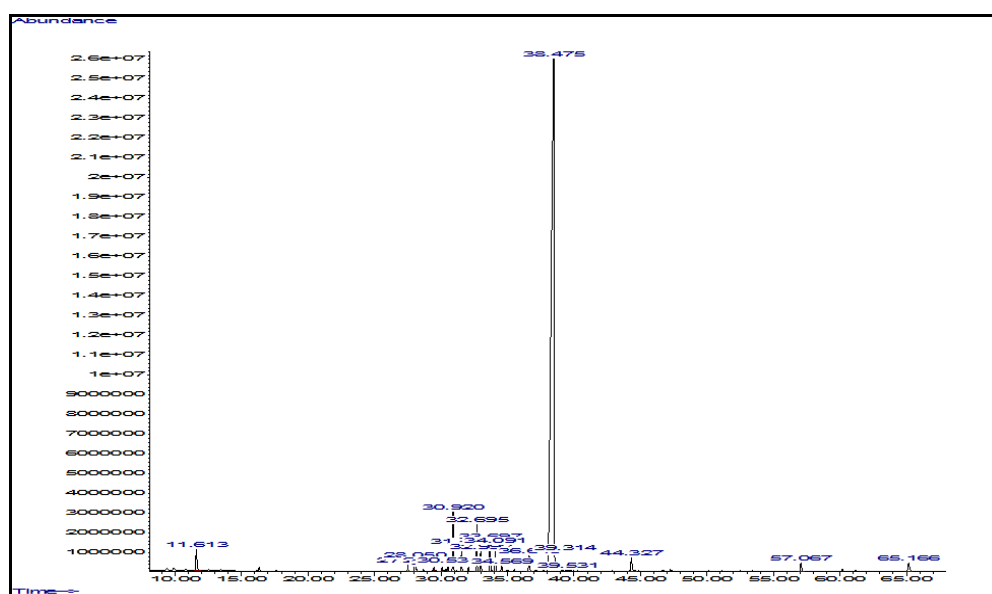
Figure 4. GC- MS chromatogram of the hexane fraction of compounds from *Salvia palaestina*

4. Conclusion

Today, more than 5000 phytochemicals have been discovered, although it varies according to plant species, most of them have not been identified yet. From current research, *Salvia palaestina*, *Alkanna trichophila* var. *mardinensis*, *Scutellaria orientalis* samples (whole plant parts) revealed that they constitute a wide range of bioactive phytochemicals with high therapeutic value. Especially, triclorfon, bis (2-ethylhexyl) pht-halate (DEHP), trans-caryophyllene molecules were found in large amounts, showing that these plants are candidate drug plant that can be used for a apoptosis inhibitor, an androstane receptor agonist and a plasticizer, anti-leukaemic, anti-mutagenic, antimicrobial and cytotoxic activity, insecticide, antibacterial and antifungal purposes. However, we are of the opinion that isolation of individual phytochemical components and subjecting them to pharmacological activity would certainly yield fruitful results.

The compliance to the Research and Publication Ethics: This study was carried out in accordance with the rules of research and publication ethics.

References

[1] Güner, A., Özhatay, N., Ekim, T., Başer, KHC. (editors). *Flora of Turkey and the East Aegean Islands (Suppl. 2)*, Vol. 11. Edinburgh, UK: Edinburgh University Press. 2000.

[2] Acıbuca, V and Bostan, Budak D., "Dünya'da ve Türkiye'de Tıbbi ve Aromatik Bitkilerin Yeri ve Önemi", *Çukurova Journal of Agricultural and Food Sciences*, 33(1), 37-44, 2018.

[3] Başer, H.C., "Sustainable Wild Harvesting of Medicinal and Aromatic Plants: An Educational Approach, Harvesting On Non-Wood Forest Products", Seminar Proceedings, Menemen-İzmir, Turkey, 2000.

[4] Bayramoğlu, M.M, Toksoy, D., Şen, G., "Türkiye'de Tıbbi Bitki Ticareti", II. Ormancılıkta Sosyo-Ekonomik Sorunlar Kongresi, 19-21 Şubat, SDÜ, Isparta, 2009.

[5] Mojab, F., Kamalinejad, M., Ghaderi, N., Vahidipour, H.R,. "Phytochemical screening of some species of Iranian plants", *Iranian Journal of Pharmaceutical Research*, 2(2), 77-82, 2003.

[6]   Davis, P.H., Milli, R.R., Kit, Tan. , *Flora of Turkey and The East Aegean Island (Supplement)*, Edinburgh Univ. Press., Vol. 10, Edinburgh, 1988.

[7]   Davis, P.H., *Flora of Turkey and The Aegean Islands,* University Pres, Vol: VI, Edinburg, 1978.

[8]   Wei, G., Hui, C., Lin, K., Xue-ru, L., Chao-ying, M. and He-zhong, J., " Composition And Bioactivity of the Essential Oil from the Leaves of *Lindera setchuenensis*", *Chemistry of Natural Compounds*, 52 (3), 520-522, 2016.

[9]   Molnár, P. B., Csengele, B., Erdei, A. L., Takeshi, F., Pál, V., Katalin, J. J. And Kárpáti, Z., " Identification of the Female-Produced Sex Pheromone of an Invasive Greenhouse Pest, the European Pepper Moth (Duponchelia fovealis)", *Journal of Chemical Ecology*, 44, 257-267, 2018.

[10]   Teal, J. P. E.A., . Tumlinson, R. H.. Heath, R., "Chemical and behavioral analyses of volatile sex pheromone components released by calling Heliothis virescens (F.) females (Lepidoptera: Noctuidae)", *Journal of Chemical Ecology,* 12 (1), 107-126, 1986.

[11]   Ulitzur, S. and Hastings, J. W., "Evidence for tetradecanal as the natural aldehyde in bacterial bioluminescence". *Proceedings of the National Academy of Sciences of the United States of America,* 76(1), 265-267, 1979.

[12]   Chung, I.M., Ahmad, A., Kim, S.J., Naik, P.M., Nagella, P., "Composition of the essential oil constituents from leaves and stems of Korean Coriandrum sativum and their immunotoxicity activity on the Aedes aegypti L.", *Immunopharmacology and Immunotoxicology*, 34(1), 152-6, 2012.

[13]   Černohlávková, J., Jarkovský, J., Jiří, H., "Effects of fungicides mancozeb and dinocap on carbon and nitrogen mineralization in soils", *Ecotoxicology and Environmental Safety*, 72 (1), 80-85, 2009.

[14]   Habib, M. R., Karim, M. R. "Antimicrobial and Cytotoxic Activity of Di-(2-ethylhexyl) Phthalate and Anhydrosophoradiol-3-acetate Isolated from Calotropis gigantea (Linn.) Flower", *Journal Mycobiology*, 37 (1), 31-36, 2009.

[15]   Lee, K. H., Kim, J. H., Lim, D. S., Kim, C. H., "Anti-leukaemic and Anti-mutagenic Effects of Di(2-ethylhexyl)phthalate Isolated from Aloe vera Linne", *Journal of Pharmacy and Pharmacology*, https://doi.org/10.1211/0022357001774246, 2010.

[16]   Otuki, M. F., Ferreira, J., Lima, F. V., Meyre-Silva, C., Malheiros, A., Muller, L. A., Cani, G.S., Santos, A. R.S., Yunes, R. A., Calixto, J. B., "Antinociceptive properties of mixture of alpha-amyrin and beta-amyrin triterpenes: evidence for participation of protein kinase C and protein kinase A pathways", *Journal of Pharmacology and Experimental Therapeutics*, 313(1), 310-318, 2005.

[17]   Pinto, S. A. H., Pinto, L. M. S., Guedes, M. A., Cunha, G. M. A., Chaves, M. H., Santos, F. A., Rao, V. S., "Antinoceptive effect of triterpenoid alpha,beta-amyrin in rats on orofacial pain induced by formalin and capsaicin", *Phytomedicine*, 15(8), 630-634, 2008.

[18]   Ma, J., Lu, N., Qin, W., Xu, R., Wang, Y., Chen, X., "Differential responses of eight cyanobacterial and green algal species, to carbamate insecticides", *Ecotoxicology and Environmental Safety*, 63 (2), 268-274, 2006.

[19]   Bakthavatsalam, N., Tandon, P.L., Bhagat, D., *Trichogrammatids: Behavioural Ecology". In: Sithanantham S., Ballal C., Jalali S., Bakthavatsalam N. (eds) Biological Control of Insect Pests*

Using Egg Parasitoids. Springer, New Delhi. https://doi.org/10.1007/978-81-322-1181-5_5., 2013.

[20] Tao, C., Wu, J., Liu, Y., Liu, M., Yang, R. and Zhaolin Lv., "Antimicrobial activities of bamboo (Phyllostachys heterocycla cv. pubescens) leaf essential oil and its major components", *European Food Research and Technology*, 244, 881-891, 2018.

[21] Khatua, S., Pandey, A. and Biswas, S. J., "Phytochemical evaluation and antimicrobial properties of Trichosanthes dioica root extract", *Journal of Pharmacognosy and Phytochemistry*, 5(5), 410-413, 2016.

[22] Bakr, R. O., El-Naa, M. M., Zaghloul, S. S. and Omar, M. M., *BMC Complementary Medicine and Therapies*, 17, 1-13, 2017.

[23] Paul, A.V.N., Singh, S. and Singh, A.K. "Kairomonal effect of some saturated hydrocarbons on the egg parasitoids, Trichogramma brasiliensis (Ashmead) and Trichogramma exiguum (Hymenoptera: Trichogrammatidae)", *Journal of Applied Entomology*, 126, 409-416, 2002.

[24] Rizwan, K., Zubair, M , Rasool, N. , Riaz, M., Zia-Ul-Haq, M. and de Feo, V., "Phytochemical and Biological Studies of Agave attenuata", *International Journal of Molecular Sciences*, 13, 6440-6451, 2012.

[25] Gumgumjee, N.M. and Hajar, S.A. "Antibacterial activities and GC-MS analysis of phytocomponents of Ehretia abyssinica R.Br. ex fresen" *International Journal of Applied Biology and Pharmaceutical Technology*, 6(2), 236-241, 2015.

[26] Habib, R., Karim M. R., "Antitumour evaluation of di-(2-ethylhexyl) phthalate (DEHP) isolated from Calotropis gigantea L. flower", *Acta Pharmaceutica*, 62(4), 607-615, 2012.

[27] Drapeau, J., Verdier, M., Touraud, D., Kröckel, U., Geier, M., Rose, A., Kunz, W., "Effective insect repellent formulation in both surfactantless and classical microemulsions with a long-lasting protection for human beings", *Chemistry & biodiversity*, 6(6), 934-47, 2009.

[28] Accession adress: "http://fses.oregonstate.edu/", accession date 01.12.2020.

[29] Öztürk, M., Duru, M. E., Aydoğmuş-Öztürk, F., Harmandar, M. , Mahlıçlı, M., Kolak, U. and Ulubelen, A., "GC-MS Analysis and Antimicrobial Activity of Essential Oil of Stachys cretica subsp. smyrnaea", *Natural Product Communications*, 4 (1), 109-114, 2009.

[30] Park, S,Y,, Park, S.J., Park, N.J., Joo, W.H., Lee, S.J., Choi, Y.W., "α-Iso-cubebene exerts neuroprotective effects in amyloid beta stimulated microglia activation", *Neuroscience Letters*, Oct 25;555:143-148. doi: 10.1016/j.neulet. 09.053, 2013.

[31] Kwon, B., Shin, H., Moon, H.B., Ji, K., Kim, K.T., "Effects of tris(2-butoxyethyl) phosphate exposure on endocrine systems and reproduction of zebrafish (Danio rerio)", *Environmental Pollution*, 214, 568-574, 2016.

[32] Sharififar, F., Mozaffarian, V., Moradkhani, S., "Comparison of antioxidant and free radical scavenging activities of the essential oils from flowers and fruits of Otostegia persica Boiss", *Pakistan Journal of Biological Sciences*, 10(21), 3895-3899, 2007.

[33] Lin, X.H., Wu, Y.B., Lin, S. Zeng, J.W., Zeng, P.Y., Wu, J.Z. "Effects of volatile components and ethanolic extract from Eclipta prostrata on proliferation and differentiation of primary osteoblasts", *Molecules*, 15(1), 241-50, 2010.

[34]Sivasubramanian, R. and Brindha, P. "In- vitro cytotoxic, antioxidant and GC-MS studies on Centratherum punctatum cass.", *International Journal of Pharmacy and Pharmaceutical Sciences*, 5(3), 364-367, 2013.

[35] Islam, S., Firoz, M., "Triacontanol as a dynamic growth regulator for plants under diverse environmental conditions ", *Physiology and Molecular Biology of Plants*, 26(5), 871-883, 2020.

[36] Kuiate, J.R., Bessière, J.M., Zollo, P.H., Kuate, S.P., "Chemical composition and antidermatophytic properties of volatile fractions of hexanic extract from leaves of Cupressus lusitanica Mill. from Cameroon", *Journal of Ethnopharmacology*, 103(2), 160-165, 2006.

[37] Kumar, S., Malhotra, R., Kumar, D., "Euphorbia hirta: Its chemistry, traditional and medicinal uses, and pharmacological activities", *Pharmacognosy Reviews*, , 4(7), 58-61, 2010.

[38] Jemia, M.B., Formisano, C., Bancheva, S., Bruno, M., Senatore, F., "Chemical composition of the essential oils of Centaurea formanekii and C. orphanidea ssp. thessala, growing wild in Greece", *Natural product communications*, 7(8), 1083-1086, 2012.

[39] Begum, I., Faridha, R., Mohankumar, M., Jeevan, Ramani, K., "GC-MS Analysis of Bio-active Molecules Derived from Paracoccus pantotrophus FMR19 and the Antimicrobial Activity Against Bacterial Pathogens and MDROs", *Indian Journal of Microbiology*,56(4), 426-432, 2016.

[40] Zakariaa, M.B., Vijayasekarana, Ilhama, Z. and Muhamad, N.A., "Anti-Inflammatory Activity of Calophyllum inophyllum Fruits Extracts", *Procedia Chemistry,* 13, 218-222, 2014.

[41] Köse, Y.B., Iscan, G. and Demirci, B., "Antimicrobial Activity of the Essential Oils Obtained from Flowering Aerial Parts of Centaurea lycopifolia Boiss. et Kotschy and Centaurea cheirolopha (Fenzl) Wagenitz from Turkey", *Journal of Essential Oil Bearing Plants*, 19(3), 762 - 768, 2016.

[42] Yamuna, P., Abirami, P., Vijayashalini, P. and Sharmila, M., "GC-MS analysis of bioactive compounds in the entire plant parts of ethanolic extract of Gomphrena decumbens Jacq.", *Journal of Medicinal Plants Studies*, 5(3), 31-37, 2017.

[43] Öğütçü, H., Sökmen, A., Sökmen, M., Polissiou, M., Serkedjieva, J., Daferera, D., Şahin, F., Barış, Ö., Güllüce, M. "Bioactivities of the Various Extracts and Essential Oils of Salvia limbata C.A.Mey. and Salvia sclarea L." *Turkish Journal of Biology*, 32, 181-192, 2008.

[44] Mitropoulou, G., Sidira, M., Skitsa, M., Tsochantaridis, I., Pappa, A., Dimtsoudis, C., Proestos, C. And Kourkoutas, Y., "Assessment of the Antimicrobial, Antioxidant, and Antiproliferative Potential of Sideritis raeseri subps. Raeseri Essential Oil", *Foods,* 9(7), 860, 2020.

[45] Dahham, S. S., Tabana, Y. M., Iqbal, M. A., Ahamed, M. B. K., Ezzat, M.O., Aman, S. A. M. and Amin, M. S. A. M., "The Anticancer, Antioxidant and Antimicrobial Properties of the Sesquiterpene β-Caryophyllene from the Essential Oil of Aquilaria crassna", *Molecules,* 20(7), 11808-11829, 2015.

[46] Adamu, U. A., Magaji, B., Ibrahim, M. N. and San, M. M., "Synthesis, Characterization and Antibacterial Evaluation of Mn (II), Co (II) and Cu (II) Complexes of Schiff Base Derived from 3-aminophenol and Benzaldehyde", *Asian Journal of Chemical Sciences*, 7(2), 39-44, 2020.

[47] Dunier, M., Siwicki, Andrzej K., Demaël, A., "Effects of organophosphorus insecticides: Effects of trichlorfon and dichlorvos on the immune response of carp (Cyprinus carpio): III. In Vitro effects on lymphocyte proliferation and phagocytosis and in vivo effects on humoral response". *Ecotoxicology and Environmental Safety*, 22 (1), 79-87, 1991.

[48] Daisy, B. H., Strobel, G. A., Castillo, U., Ezra, D., Sears, J. , Weaver, D. K., Runyon, J. B., "Naphthalene, an insect repellent, is produced by Muscodor vitigenus, a novel endophytic fungus", *Microbiology (Reading)*, 148 (11), 3737-3741, 2002.

[49] Matolcsy, G., Nádasy, M., Andriska, V., *Pesticide chemistry,*.Amsterdam-Oxford-New York-Tokyo, 551, 1988.

[50] Accession adress: https://drugs.ncats.io/drug/, accession date 01.12.2020.

Middle East Journal of Science

Research Article

A HYBRID MULTI-CRITERIA DECISION MAKING METHOD FOR ROBOT SELECTION IN FLEXIBLE MANUFACTURING SYSTEM

Shafi Ahmad[1] ID   **Sedat Bingol[2]* ID   *Saif Wakeel [3]* ID

[1]Department of Mechanical Engineering, Jamia Millia Islamia, New Delhi-110025, India
[2]Department of Mechanical Engineering, Dicle Universitesi, Diyarbakir, Turkey
[3]Centre of Advanced Materials, Department of Mechanical Engineering University of Malaya, Kuala Lumpur, Malaysia

* Corresponding author; sbingol@dicle.edu.tr

Abstract: *Advancement of the manufacturing system is governed by robots which improve the product quality and decrease market availability period. Different robots have been used for the pick and drop the operation of components in flexible manufacturing systems (FMS). Each robot have their advantages and disadvantages therefore, selection of the most suitable robot is significantly important. The selection of robots based on various criteria is a multi-decision making problem (MCDM). In this study seven robots (R1, R2, R3, R4, R5, R6, R7) are ranked using the proposed approach on the basis of five criteria viz. load capacity (L_C), memory capacity (M_C), manipulator reach (M_R), maximum tip speed (M_{TS}), and repeatability (R_E) by employing hybrid Criteria Importance Through Inter criteria Correlation (CRITIC) and Multi-attributive border approximation area comparison (MABAC) methods. Weights of criteria were obtained using correlation coefficient and standard deviation method whereas, the ranking of alternative was done using hybrid CRITIC and MABAC method. As a result of this study, robot R3 acquired the first rank whereas, R1 occupied the last rank which showed that R3 is the most suitable robot for the pick and place operation in FMS. Besides, Ranking comparison was also done with other MCDM methods.*

1. Introduction

An activated instrument with a level of independence, programmable in more than one axis used to execute deliberated operations is known as a robot. The term independence defines the capability of a robot to execute projected operations within the existing conditions and sensing, exclusive of human interference. In this regard, robots overpass the breach among mechanical instruments and human operators. They are considered to execute repetitious, complex, and dangerous operations in an accurate manner for eminence, production, and safety reasons [1], [2]. Due to which they have been expansively accepted to execute different operations. In the last decade, a hot-headed escalation of robot implementation in flexible manufacturing systems (FMS) and automatic storage and retrieval systems (AS/RS) have been observed. However, the use of a robot in manufacturing systems has a significant impact on the company. As the cost of these robots is generally high, using an inappropriate robot in the manufacturing system will unfavorably influence the productivity and efficiency of the system [1], [2].

Hence, in order to improve the efficiency and productivity of entire manufacturing systems, an appropriate selection of industrial robots is vital [3], [4]. With the advancement of information technology and computer science, there are a large number of robots with enormously diverse stipulations and potential for a variety of application fields [5]. In such conditions, the selection of a qualified robot among a variety of existing alternatives is a very difficult task for decision-makers [2].

Robot selection is reasonably complex because of the convolution, characteristics, quality, and capabilities of different robots that are constantly improved [6]. Additionally, the incompatible characteristics and capabilities of some robots complicate the decision-making process. It has been found that there exist a large number of criteria that should be reckoning while selecting a robot to perform desired operations [5]. However, it is very difficult to consider all the criteria simultaneously while selecting an appropriate robot for the desired output. This entails that multiple criteria decision making (MCDM) methods might be helpful to solve this kind of problem. The solution to the robot selection process starts with the identification of the appropriate evaluation criteria and thereby prioritizing these criteria using MCDM methods. Subsequently, the best amalgamation of these criteria is used to select a qualified robot among the available robots in the market [7].

Over the years researchers have used different MCDM methods to solve robot selection problems [13, 14]. This work put forward a hybrid MCDM model based on Criteria Importance Through Inter criteria Correlation (CRITIC) and Multi-attributive border approximation area comparison (MABAC) methods. The viability of the proposed approach is demonstrated by employing the proposed approach to select an appropriate robot for pick and place operation. Pick and drop operation in an FMS is usually performed by automated guided vehicles (AGVs) which are a specific type of robot used for picking and placing part at the desired location. Seven robots are ranked using the proposed approach on the basis of five criteria viz. load capacity (LC), memory capacity (MC), manipulator reach (MR), maximum tip speed (MTS), and repeatability (RE) [8]. The rest of the paper is organized as follows: Section 2 of the paper describes the proposed approach to solve the robot selection problem. The computations steps involved in CRITIC and MABAC methods are also discussed in this section. Section 3 of the paper depicts the results of the study. The comparison of the ranking results of the proposed method with previous methods is also shown in this section to validate the results of the study. Finally, Section 4 of the paper presents the conclusion of this study.

2. 2. Proposed MCDM model for robot selection

The proposed MCDM model to solve the robot selection problem has been depicted in the form of a flowchart in Figure 1.

At first, alternative robots for the desired application are identified. It is likely that each robot has different properties for the different attributes. Hence, significant attributes for the evaluation of the robots are identified. Further, CRITIC method which is a widely used MCDM tool for calculation of criteria weight is employed to calculate the weights of the criteria. Using the weights of the criteria and the properties of robots, the MABAC method is employed to rank the identified robots.

The Criteria Importance Through Inter criteria Correlation (CRITIC) method was proposed by [9]. This method computes the objective weight of the attributes on the basis of two fundamental notions of MCDM viz. Contrast intensity and conflict among the attributes. It has been established that the weight of the attributes obtained using CRITIC method is identical with PCA with simple computations steps [9]. The Multi-Attribute Border Approximation area Comparison (MABAC) method was developed in 2015 and is effectively employed to solve problems pertaining to different knowledge

domains [10]–[12]. In this method, ranks to the alternatives are defined on the basis of their distance from the border approximation area. An alternative having the highest distance from the border approximation area is ranked first and subsequently ranks to other alternatives are defined in descending values of their distance from the border approximation area.

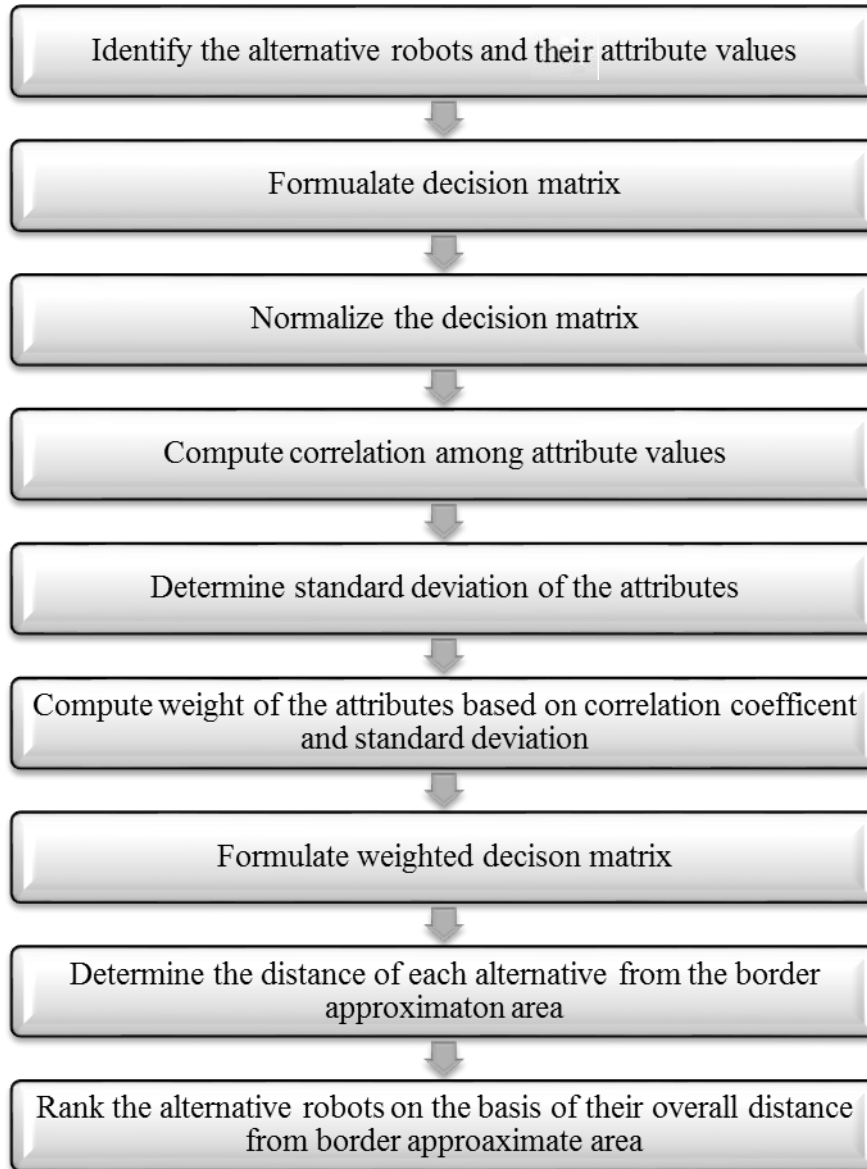**Figure 1**. Proposed MCDM model for robot selection

The computational steps involved in the proposed MCDM model for robot selection are discussed as follows:

Step 1: Formulate decision matrix by arranging alternative robots and their attribute values in rows and columns. Assuming there are *"p"* alternative robots and *"q"* decision attributes. The decision matrix *(DM)* can be formulated as shown in Eq. (1):

$$DM = \left[a_{ij}\right]_{p \times q} = \begin{bmatrix} a_{11} & a_{12} & \dots & a_{1j} & \dots & a_{1q} \\ a_{21} & a_{22} & \dots & \dots & \dots & a_{2q} \\ \dots & \dots & \dots & \dots & \dots & \dots \\ a_{i1} & \dots & \dots & a_{ij} & \dots & a_{iq} \\ \dots & \dots & \dots & \dots & \dots & \dots \\ a_{p1} & \dots & \dots & a_{pj} & \dots & a_{pq} \end{bmatrix}$$

where its elements a_{ij} represents the value of the jth decision attribute for ith alternative robot. i = 1,2,3,……..,p; j = 1,2,3,………….,q.

Step 2: Normalize the decision matrix to convert the distinct range of attribute values into a comparable range. Since attributes can be of different nature viz. beneficial and non-beneficial, they are normalized using Eq. (2) according to their nature.

$$n_{ij} = \begin{cases} \dfrac{a_{ij} - \min\limits_{i}(a_{ij})}{\max\limits_{i}(a_{ij}) - \min\limits_{i}(a_{ij})} ; & if\ j \in beneficial\ attribute \\ \dfrac{\max\limits_{i}(a_{ij}) - a_{ij}}{\max\limits_{i}(a_{ij}) - \min\limits_{i}(a_{ij})} ; & if\ j \in non\ beneficial\ attribute \end{cases} \tag{2}$$

where nij indicates the normalized value of the ith alternative for jth attribute.
Step 3: Determine the Correlation Coefficient (ρ_{jk}) among all the attributes using Eq. (3).

$$\rho_{jk} = \frac{\sum_{i=1}^{p}(n_{ij} - \overline{n}_j)(n_{ik} - \overline{n}_k)}{\sqrt{\sum_{i=1}^{p}(n_{ij} - n_j)^2 * \sum_{i=1}^{p}(n_{ik} - \overline{n}_k)^2}} \tag{3}$$

Step 4: Determination of the standard deviation of the attributes (σ_j) as defined by Eq. (4)

$$\sigma_j = \sqrt{\frac{1}{q-1}\sum_{j=1}^{q}(n_{ij} - \overline{n}_j)^2} \tag{4}$$

Step 5: Compute the amount of information provided by each attribute (Aj) using Eqn. (5)

$$A_j = \sigma_j \sum_{j=1}^{q}\left(1 - \rho_{jk}\right) \tag{5}$$

Step 6: Compute the weight of the attributes using Eqn. (6).

$$w_j = \frac{A_j}{\sum_{j=1}^{n} A_j} \tag{6}$$

It must be ensured that all weights add up to 1.

Step 7: Determine weighted normalized decision matrix W = [vij]p×q.

$$W = \left[v_{ij}\right]_{p \times q} = \begin{bmatrix} v_{11} & v_{12} & ... & v_{1j} & ... & v_{1q} \\ v_{21} & v_{22} & ... & ... & ... & v_{2q} \\ ... & ... & ... & ... & ... & ... \\ v_{i1} & ... & ... & v_{ij} & ... & v_{iq} \\ ... & ... & ... & ... & ... & ... \\ v_{p1} & ... & ... & v_{pj} & ... & v_{pq} \end{bmatrix} \qquad (7)$$

where, vij = (nij+1)×wj.

Step 8: Determine the border approximation area of each attribute as defined by Eqn. (8).

$$B_j = \left(\prod_{i=1}^{p} v_{ij}\right)^{1/p} \qquad (8)$$

Step 9: Compute total distance of each alternative from the border approximation area as given by Eqn. (9).

$$S_i = \sum_{j=1}^{q} r_{ij} \qquad (9)$$

where, rij = vij − Bj

Step 10: Rank the alternatives based on Si values in ascending order. An alternative with the minimum Si value is ranked first and an alternative with the highest value is ranked last.

3. Additional instructions

To demonstrate the potential application of the proposed MCDM model to solve the robot selection problem, it has been employed on a specific problem chosen from the literature [5]. Every manufacturing company requires a robot for picking parts and placing them in the right place. Hence, the selection of an appropriate robot for performing these operations is imperative. Five criteria are used for the selection of these types of robots i.e. load capacity (L_C), memory capacity (M_C), manipulator reach (M_R), maximum tip speed (M_{TS}), and repeatability (R_E). These criteria are defined as follows:

- Load capacity (L_C): It is the maximum load that a manipulator can carry without affecting the performance.
- Memory capacity (M_C),: It is the number of points or steps that a robot can store in its memory while traveling along its predetermined path.
- Manipulator reach (M_R): It is the maximum distance that can be covered by the robotic manipulator so as to grasp the object for the given pick-and-place operation.
- Maximum tip speed (M_{TS}): It is the speed at which a robot can move in an inertial reference frame
- Repeatability (R_E): It measures the ability of a robot to return to the same position and orientation over and over again.

Among these criteria, L_C, M_{TS}, M_C, and M_R are benefit-type criteria, and R_E is a cost-type criterion. Seven robots have been identified which are widely used in the industry for pick and place operations. The criteria values of these robots are shown in Table 1.

Table 1. Attribute Values for different robots

Robot	L_C (kg)	M_C	M_R (mm)	M_{TS} (mm/s)	R_E (mm)
ROB$_1$	6	500	990	2540	0.4
ROB$_2$	6.35	3000	1041	1016	0.15
ROB$_3$	6.8	1500	1676	1727.2	0.1
ROB$_4$	10	2000	965	1000	0.2
ROB$_5$	2.5	500	915	560	0.1
ROB$_6$	4.5	350	508	1016	0.08
ROB$_7$	3	1000	920	177	0.1

Since the first step in the proposed MCDM model is to formulate a decision matrix. Table 1 acts as a decision matrix for this robot selection problem. The attribute values provided in Table 1 are normalized as per Eqn. (2) and the normalized values are depicted in Table 2:

Table 2. Normalized attribute

	LC	RE	MTS	MC	MR
R1	0.5333	1.0000	0.0000	0.9434	0.5873
R2	0.4867	0.2188	0.6449	0.0000	0.5437
R3	0.4267	0.0625	0.3440	0.5660	0.0000
R4	0.0000	0.3750	0.6517	0.3774	0.6087
R5	1.0000	0.0625	0.8379	0.9434	0.6515
R6	0.7333	0.0000	0.6449	1.0000	1.0000
R7	0.9333	0.0625	1.0000	0.7547	0.6473

Further, the correlation coefficient and standard deviation of the attributes are computed using Eqn. (3) and Eqn. (4) as per step 3 and step 4 of the proposed model. On the basis of the correlation coefficient and standard deviation, the amount of information and weights of the attributes are computed using Eqn. (5) and Eqn. (6) and are exhibited in Table 3.

Subsequently, the weighted normalized decision matrix is formulated as defined by Eqn. (7). Table 4 represents the weighted normalized decision matrix so formulated.

Correspondingly, the border approximation area for each attribute is determined as defined by Eqn. (8). Finally, the ranking of the alternative robot is done on the basis of the sum of the distance of each alternative from the border approximate area computed using Eqn. (9). Table 5 exhibit the Si values and the rank of the alterative robot so obtained.

Table 3. Amount of information and weight of the attributes.

Attribute	A	Weight
LC	1.0361	0.1679
RE	1.7854	0.2893
MTS	1.3411	0.2173
MC	1.1287	0.1829
MR	0.8790	0.1424

Table 4. Weighted normalized decision matrix

	LC	**RE**	**MTS**	**MC**	**MR**
R1	0.2575	0.5787	0.2173	0.3555	0.2261
R2	0.2496	0.3526	0.3575	0.1829	0.2199
R3	0.2396	0.3074	0.2921	0.2865	0.1425
R4	0.1679	0.3979	0.3590	0.2520	0.2292
R5	0.3358	0.3074	0.3995	0.3555	0.2353
R6	0.2910	0.2894	0.3575	0.3659	0.2849
R7	0.3246	0.3074	0.4347	0.3210	0.2347

Table 5. Si and rank of the alternative robots

	Si	Rank
R1	0.1671	7
R2	-0.1053	2
R3	-0.1999	1
R4	-0.0621	3
R5	0.1654	6
R6	0.1206	4
R7	0.1543	5

Further, the ranking results of the proposed MCDM model are compared with that of the ranking results given by other researchers [6]. Figure 2 shows the comparison of the ranking results for all the seven robots using VIKOR, ELECTREII, and the proposed model.

It can be observed from Figure 2 that the ranking results for the robots vary for all three methods. It is quite obvious as the approach adopted is different and it is difficult to suggest the best method among the available MCDM method. However, the proposed approach suggests ROB_3 is the best robot which is in line with the results of the other methods. Hence, the proposed method can be profitably used to solve the robot selection problem.
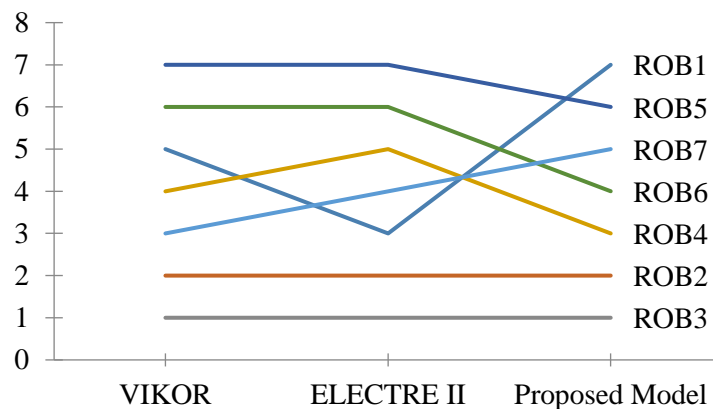
Figure 2. Comparison of the ranking results

4. Conclusions

The selection of appropriate robots for desired operations in manufacturing systems is very difficult for decision-makers as there exist a number of different robots with a variety of characteristics and features. The problem of robot selection can be solved using MCDM methods. In this study, a hybrid MCDM method combining CRITIC and MABAC method has been employed to rank the robots used in manufacturing facilities. Weights of all the criteria were calculated using correlation coefficient and standard deviation methods and then, the ranking of seven alternatives was done. Besides, ranking results were also compared with widely used methods such as VIKOR and ELECTRE II. Based on the results obtained in this study, the following major conclusions are made.

1. Most suitable robot ranking sequence obtained using the CRITIC and MABAC method is R3>R2>R4>R6>R7>R5>R1.

2. Robot 3 is the most suitable alternative for pick and drop mechanism as it has the highest manipulator reach, optimum load capacity along with higher maximum tip speed and lower repeatability. Whereas, Robot 7 is the least favorable choice.

3. Ranking obtained using the VIKOR and ELECTRE II methods were similar to the hybrid method applied in this study which supported the reliability and consistency of the CRITIC and MABAC methods.

The compliance to the Research and Publication Ethics: This study was carried out in accordance with the rules of research and publication ethics.

References

[1] R. Kumar and R. K. Garg, "Optimal selection of robots by using distance-based approach method," *Robotics and Computer-Integrated Manufacturing*, vol. 26, no. 5, pp. 500–506, Oct. 2010, doi: 10.1016/j.rcim.2010.03.012.

[2] R. V. Rao, B. K. Patel, and M. Parnichkun, "Industrial robot selection using a novel decision-making method considering objective and subjective preferences," *Robotics and Autonomous Systems*, vol. 59, no. 6, pp. 367–375, Jun. 2011, doi: 10.1016/j.robot.2011.01.005.

[3] D. E. Koulouriotis and M. K. Ketipi, "Robot evaluation and selection Part A: an integrated review and annotated taxonomy," *Int J Adv Manuf Technol*, vol. 71, no. 5–8, pp. 1371–1394, Mar. 2014, doi: 10.1007/s00170-013-5525-5.

[4] M. K. Ketipi, D. E. Koulouriotis, and E. G. Karakasis, "Robot evaluation and selection Part B: a comparative analysis," *Int J Adv Manuf Technol*, vol. 71, no. 5–8, pp. 1395–1417, Mar. 2014, doi: 10.1007/s00170-013-5526-4.

[5] P. P. Bhangale, V. P. Agrawal, and S. K. Saha, "Attribute based specification, comparison and selection of a robot," *Mechanism and Machine Theory*, vol. 39, no. 12, pp. 1345–1366, Dec. 2004, doi: 10.1016/j.mechmachtheory.2004.05.020.

[6] P. Chatterjee, V. Manikrao Athawale, and S. Chakraborty, "Selection of industrial robots using compromise ranking and outranking methods," *Robotics and Computer-Integrated Manufacturing*, vol. 26, no. 5, pp. 483–489, Oct. 2010, doi: 10.1016/j.rcim.2010.03.007.

[7] A. Kentli and A. K. Kar, "A satisfaction function and distance measure based multi-criteria robot selection procedure," *International Journal of Production Research*, vol. 49, no. 19, pp. 5821–5832, Oct. 2011, doi: 10.1080/00207543.2010.530623.

[8] Y. Fu, M. Li, H. Luo, and G. Q. Huang, "Industrial robot selection using stochastic multicriteria acceptability analysis for group decision making," *Robotics and Autonomous Systems*, vol. 122, p. 103304, Dec. 2019, doi: 10.1016/j.robot.2019.103304.

[9] D. Diakoulaki, G. Mavrotas, and L. Papayannakis, "Determining objective weights in multiple criteria problems: The critic method," *Computers & Operations Research*, vol. 22, no. 7, pp. 763–770, Aug. 1995, doi: 10.1016/0305-0548(94)00059-H.

[10] D. I. Božanić, D. S. Pamučar, and S. M. Karović, "Application the MABAC method in support of decision-making on the use of force in a defensive operation," *Tehnika*, vol. 71, no. 1, pp. 129–136, 2016.

[11] D. Pamučar, Ž. Stević, and E. K. Zavadskas, "Integration of interval rough AHP and interval rough MABAC methods for evaluating university web pages," *Applied Soft Computing*, vol. 67, pp. 141–163, 2018.

[12] D. Pamučar and G. Ćirović, "The selection of transport and handling resources in logistics centers using Multi-Attributive Border Approximation area Comparison (MABAC)," *Expert systems with applications*, vol. 42, no. 6, pp. 3016–3028, 2015.

[13] Wakeel, S., Bingol, S., Bashir, M. N., & Ahmad, S. (2020). Selection of sustainable material for the manufacturing of complex automotive products using a new hybrid Goal Programming Model for Best Worst Method–Proximity Indexed Value method. *Proceedings of the Institution of Mechanical Engineers, Part L: Journal of Materials: Design and Applications*, 1464420720966347.

[14] Wakeel, S., Ahmad, S., Bingol, S., Bashir, M. N., Paçal, T. C., & Khan, Z. A. (2020, August). Supplier Selection for High-Temperature Die Attach by hybrid Entropy-Range of Value MCDM Technique: A Semiconductor Industry. In *2020 21st International Conference on Electronic Packaging Technology (ICEPT)* (pp. 1-5). IEEE

Research Article

NEW EXACT SOLUTIONS FOR KLEIN-GORDON EQUATION

Faruk Düşünceli^{*1} (ID)

¹ Mardin Artuklu University Departmant of Economics
[*] Corresponding author; farukdusunceli@artuklu.edu.tr

Abstract: *In this paper, we applied the improved Bernoulli sub-equation function method for the Klein-Gordon equation. Firstly, we reduced the equation to a nonlinear ordinary differential equation with the aid of wave transform. Then we obtained various new exact solutions via the method. These solutions can play an important role in engineering and physics. For some solutions, we drew two and three-dimensional graphics to understand physical behaviors. We performed all the calculations and graphs in this article by Wolfram Mathematica.*
Keywords*: Klein-Gordon Equation, Improved Bernoulli sub-equation function method, Exact solutions.*

1. Introduction

Nonlinear evolution equations (NLEEs) are widely used because it finds application in many nonlinear disciplines such as plasma physics, optical fibers, fluid mechanics, fluid dynamics[1-4] and so on. One of the best known of these equations is Klein-Gordon equation (KGE). KGE, the relative wave equation version of Schrödinger equation, is a relative field equation for scalar particles (spin-zero) [5].
Sassaman and Biswas[5,6] investigated the general form of the perturbed KGE,

$$u_{tt} - u_{xx} + f(u) = \varepsilon(\alpha u + pu_t + qu_x + \beta u_{xt} + \gamma u_{tt}) \tag{1},$$

where $\alpha, \beta, \gamma, p, q$ are constants and ε is the perturbation parameter. Zhang [7] investigated this equation without local inductance and dissipation effect:

$$u_{tt} - u_{xx} + f(u) = \varepsilon(\alpha u + \beta u_{xt} + \gamma u_{tt}) \tag{2}$$

When $f(u) = au - bu^2$ and $\varepsilon = 0$, Eq.(1) degrades the KGE with quadratic nonlinearity:

$$u_{tt} - u_{xx} + au - bu^2 = 0 \tag{3}$$

When $f(u) = au - bu^3$ and $\varepsilon = 0$, Eq.(1) degrades the KGE with cubic nonlinearity:

$$u_{tt} - u_{xx} + au - bu^3 = 0 \tag{4}$$

Equation (4) has been solved by many different methods in the literature. Zhang [8] used the trigonometric function series method. Wazwaz[9] applied the tanh and sine-cosine methods. Hafez et al. [10] solved it with $\frac{G'}{G}$ expansion method. Yindoula et al. [11] solved it with He-Laplace and the Decomposition Laplace-Adomian method. Lastly, Shahen et al. [12] used the $\exp(-\varphi(\varepsilon))$expansion method.

In this paper, we solved equation (4) by improved Bernoulli sub-equation function method (IBSEFM). The remainder of this paper is prepared as follows: In section 2, the method has been discussed. In section 3, we applied this method to the KGE with cubic nonlinearity. Lastly, conclusions are given in section 4.

2. Material and method

Improved Bernoulli sub-equation function method [13-17] formed by modifying the Bernoulli sub-equation function method will be introduced in this section. The algorithm below should be applied sequentially.

1. Let's consider the following partial differential equation;

$$P(u, u_x, u_{y,} \dots, u_{xx}, u_{xy}, \dots = 0, \tag{2}$$

and take the wave transformation;

$$u(x, y, t, \dots) = U(\eta), \quad \eta = kx + ly + mt + \cdots \tag{3}$$

where $k, l, m, \dots$ are constants and will be determined later. Putting Equation (3) in Equation (2), we get the following nonlinear ordinary differential equation;

$$N\left(U, U', U'', U''', \cdots\right) = 0. \tag{4}$$

2. Considering the trial equation in Equation (4), it can be written as follows;

$$U(\eta) = \frac{\sum_{i=0}^{n} a_i F^i(\eta)}{\sum_{j=0}^{m} b_j F^j(\eta)} = \frac{a_0 + a_1 F(\eta) + a_2 F^2(\eta) + \cdots + a_n F^n(\eta)}{b_0 + b_1 F(\eta) + b_2 F^2(\eta) + \cdots + b_m F^m(\eta)} \tag{5}$$

According to Bernoulli theory, we can consider the general form of the Bernoulli differential equation for F' as follows:

$$F' = wF + dF^M, w, d \neq 0, M \in R - \{0,1,2\} \tag{6}$$

Where $F = F(\eta)$ is Bernoulli differential polynomial. By replacing the above relations with Equation (4), it gives the equations of polynomial $\varphi(F)$ as follows;

$$\varphi(F) = \rho_s F^s + \cdots + \rho_1 F + \rho_0 = 0 \tag{7}$$

According to the balance principle, we can determine the relationship between n, m and M .

3. The coefficients of (F) must all be zero and give us an algebraic system of equations;

$$\rho_i = 0, i = 0, \cdots, s. \tag{8}$$

Solving this system, we will determine the values of $a_0, \cdots, a_n$ and $b_0, \cdots, b_m$.

4. When we solve the nonlinear Bernoulli differential equation (6), we get the following two cases with respect to w and d;

$$F(\eta) = \left[\frac{-d}{w} + \frac{E}{e^{w(1-M)\eta}}\right]^{\frac{1}{1-M}}, w \neq d \tag{9}$$

$$F(\eta) = \left[\frac{(E-1)+(E+1)\tanh(w(1-M)\frac{\eta}{2})}{1-\tanh(w(1-M)\frac{\eta}{2})}\right]^{\frac{1}{1-M}}, \ w = d, \ E \in R \tag{10}$$

3. Findings

In this section, the application of the improved Bernoulli sub-equation function method to the Klein-Gordon Equation is discussed. Using the wave transformation on equation (1)

$$\emptyset(x,t) = U(\eta), \ \eta = kx - lt \tag{11}$$

Substituting equation (11) into equation (1), gives the following NODE:

$$(l^2 + \alpha k^2)U'' + aU - bU^3 = 0 \tag{12}$$

Balancing equation (12) by considering the highest derivative (U'') and the highest power (U^3), we obtain

$$n - m = M - 1.$$

When $M = 3, m = 1,$ gives $n = 3$. Thus, the trial solution for equation (1) takes the following form:

$$U(\eta) = \frac{a_0 + a_1 F(\eta) + a_2 F^2(\eta) + a_3 F^3(\eta)}{b_0 + b_1 F(\eta)},$$ (13)

Where $F' = wF + dF^3, w \neq 0, d \neq 0$. Substituting equation (13), its second derivative along with $F' = wF + dF^3, w \neq 0, d \neq 0$ into equation (12), gives an F polynomial. Solving the system of the algebraic equations gives the values of the relevant parameter. Substituting the obtained values of the parameters into equation (13), gives the solutions to equation (1).

$w \neq d$, We can find the following coefficients:

Case 1.

$$a_1 = \frac{a_0 b_1}{b_0}; a_2 = \frac{2d a_0}{\sigma}; a_3 = \frac{2d a_0 b_1}{\sigma b_0}; w = d; c = 2(l^2 + k^2 \alpha)\sigma^2; b = -\frac{2(l^2 + k^2 \alpha)\sigma^2 b_0^2}{a_0^2};$$ (14)

Case 2.

$$a_1 = \frac{a_0 b_1}{b_0}; a_2 = 0; a_3 = 0; \alpha = -\frac{l^2}{k^2}; w = 3d; a = -\frac{b a_0^2}{b_0^2};$$ (15)

Case 3.

$$a_1 = \frac{a_0 b_1}{b_0}; a_2 \to 0; a_3 \to 0; l = -ik\sqrt{\alpha}; a = -\frac{b a_0^2}{b_0^2};$$ (16)

Substituting equation (14) into equation (13), gives

$$u_1(x,t) = \frac{a_0 + \frac{2d a_0}{(e^{-2(-lt+kx)\sigma} \mathrm{E} - \frac{d}{\sigma})\sigma} + \frac{a_0 b_1}{\sqrt{e^{-2(-lt+kx)\sigma} \mathrm{E} - \frac{d}{\sigma}} b_0} + \frac{2d a_0 b_1}{(e^{-2(-lt+kx)\sigma} \mathrm{E} - \frac{d}{\sigma})^{3/2} \sigma b_0}}{b_0 + \frac{b_1}{\sqrt{e^{-2(-lt+kx)\sigma} \mathrm{E} - \frac{d}{\sigma}}}}.$$ (17)

Substituting equation (15) into equation (13), gives

$$u_2(x,t) = \cfrac{a_0 + \cfrac{a_0 b_1}{\sqrt{e^{-2(-lt+kx)\sigma}\sigma_{\mathrm{E}} - \frac{3d}{\sigma}} - b_0}}{b_0 + \cfrac{b_1}{\sqrt{e^{-2(-lt+kx)\sigma}\sigma_{\mathrm{E}} - \frac{3d}{\sigma}}}}.$$
(18)

Substituting equation (16) into equation (13), gives

$$u_3(x,t) = \cfrac{a_0 + \cfrac{a_0 b_1}{\sqrt{e^{-2(kx+ikt\sqrt{\alpha})\sigma}\sigma_{\mathrm{E}} - \frac{w}{\sigma}} - b_0}}{b_0 + \cfrac{b_1}{\sqrt{e^{-2(kx+ikt\sqrt{\alpha})\sigma}\sigma_{\mathrm{E}} - \frac{w}{\sigma}}}}.$$
(19)

We performed numerical simulations by selecting appropriate parameter values and drawing 2D and 3D graphs of the solutions obtained for equation (17).
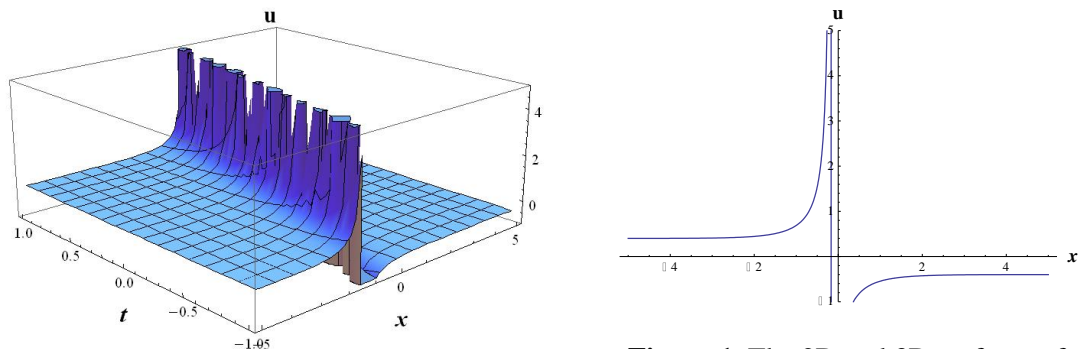
Figure 1. The 2D and 3D surfaces of the solution Eq.(17) for suitable values

4. Conclusions

IBSEF method has been employed to get new exact solutions for the Klein-Gordon Equation. When we compared the results we obtained with the previous ones, we saw that they were new solutions. The results that we obtained can be helpful in explaining the physical sense of the diverse nonlinear models that originated in the area of the nonlinear sciences. The method is a robust and efficient mathematical tool that can be used to manipulate some type of nonlinear mathematical model.. We recommend that this method can be applied to distinct nonlinear partial differential equations. We suggest applying this method to different nonlinear partial differential equations.

The compliance to the Research and Publication Ethics: This study was carried out in accordance with the rules of research and publication ethics.

References

[1] Akın, L ., "A Characterization of Approximation of Hardy Operators in VLS". *Celal Bayar University Journal of Science*, 14 (3), 333-336,2018. DOI: 10.18466/cbayarfbe.449954.

[2] Mamedov, F, Zeren, Y, Akın, L, "Compactification of weighted Hardy operator in variable exponent Lebesgue spaces", *Asian Journal of Mathematics and Computer Science*, 17:1, 38-47,2017.

[3] Akın, L. "On Some Properties of Integral-Type Operator in Weighted Herz Spaces with Variable Exponent Lebesgue Spaces" *Universal Journal of Mathematics and Applications*, 2 (3), 148-151,2019. DOI: 10.32323/ujma.522420

[4] Cruz-Uribe, D., Diening, L. and Hasto, P., "The maximal operator on weighted variable Lebesgue spaces", *Fract. Calc. Appl. Anal.* 14(3), 361-374,2011.

[5] Biswas, A., Zony, C. and Zerrad, E., "Soliton perturbation theory for the quadratic nonlinear Klein–Gordon equation" *Applied Mathematics and Computation*, 203, 153, 2008.

[6] Sassaman, R., Biswas, A, "Soliton perturbation theory for phi-four model and nonlinear Klein–Gordon equations", *Commun Nonlinear Sci Numer Simulat,* 14, 3239-3249, 2009.

[7] Zhang, Z., "Exact traveling wave solutions of the perturbed Klein–Gordon equation with quadratic nonlinearity in (1+1)-dimension, Part I: Without local inductance and dissipation effect", *Turkish Journal of Physics*, 37, 259-267,2013.

[8] Zhang, Z., "New Exact Traveling Wave Solutions for the Nonlinear Klein-Gordon Equation", *Turkish Journal of Physics*, 32, 235-240,2008.

[9] Wazwaz, A. M. "The tanh and sine-cosine methods for compact and noncompact solutions of the nonlinear Klein-Gordon equation", *Applied Mathematics and Computation*, 167(2), 1179–1195, 2005.

[10] Hafez, M. G., Nur Alam, M. and Akbar, M.A. "Exact traveling wave solutions to the Klein–Gordon equation using the novel (G0/G)-expansion method", *Results in Physics*, 4, 177-184, 2014.

[11] Yindoula, J.B., Massamba, A. and Bissanga, G., "Solving of Klein-Gordon by Two Methods of Numerical Analysis", *Journal of Applied Mathematics and Physics*, 4, 1916-1929,2016.

[12] Shahen, N.H.M., Foyjonnesa and Habibul Bashar, Md. "Exploration on traveling wave solutions to the 3rd-order klein–fock-gordon equation (KFGE) in mathematical physics", *International Journal of Physical Research*, 8(1), 14-21,2019.

[13] Baskonus H.M., Bulut H. "On the complex structures of Kundu-Eckhaus equation via improved Bernoulli sub-equation function method", *Waves in Randomand Complex Media*. 25(4) 720-728. 2015.

[14] Düşünceli, F. "Solutions for the Drinfeld-Sokolov Equation Using an IBSEFM Method", *MSU Journal of Science,* 6(1), 505-510,2018.

[15] Düşünceli, F. "New Exponential and Complex Traveling Wave Solutions to the Konopelchenko-Dubrovsky Model", *Advances in Mathematical Physics*, Article ID 7801247, 9 pages, 2019. https://doi.org/10.1155/2019/7801247.

[16] Düşünceli**,** F. "New Exact Solutions for the (3 + 1) Dimensional B-type Kadomtsev-Petviashvili Equation". *Erzincan Üniversitesi Fen Bilimleri Enstitüsü Dergisi*, 12 (1), 463-468, 2019.

[17] Düşünceli, F. Çelik, E., Aşkın, M. and Bulut, H. "New Exact Solutions for the Doubly Dispersive Equation Using an Improved Bernoulli Sub-Equation Function Method", *Indian Journal of Physics*, 1-6, 2020.

Research Article

DETERMINATION OF SUITABLE RHEOLOGICAL MODEL FOR POLYETHYLENE GLYCOLS AND SILICA PARTICLE MIXTURES

Cenk YANEN[1]   *Ercan AYDOĞMUŞ[2]*   *Murat Yavuz SOLMAZ[*3]*

[1]Department of Mechanical Engineering, Firat University, 23100 Elazig, Turkey.
[2]Department of Chemical Engineering, Firat University, 23100 Elazig, Turkey.
[3]Department of Mechanical Engineering, Firat University, 23100 Elazig, Turkey.
[*] Corresponding author: mysolmaz@firat.edu.tr

Abstract: *Shear thickening fluids are smart materials that show a sudden increase in viscosity when exceeding critical shear rates. Different theories have been proposed to explain these properties of shear thickening. The most used of these theories are Order-Disorder Transition and Hydro-Cluster Theory. Due to their reversible properties, shear thickening fluids have been used in many areas. High molecular weight polyethylene glycols showed faster shear thickening fluids behavior. The molecular weight of polyethylene glycol affects many parameters. These parameters are physical bonds, aggregations of molecular, solid particle interactions, and functional groups in the chain. Due to their effect, rheological behaviors of low and high molecular weight polyethylene glycols differ. The mixtures of polyethylene glycols and fumed silica particles show a colloidal distribution. The distribution of fumed silica particle molecules in polyethylene glycol, interaction with each other restriction, and movement of the bulks have affected rheological properties. Physical interactions are manifested in the structure. The mixture showed non-Newtonian behavior in the first and second regions as well. Rheological behaviors of mixtures were compared with experimental data using non-Newtonian models. Power Law, Bingham, Casson, Herschel-Bulkley, and Sisko model equations were used. Silica particle-PEGs mixtures show pseudo plastic in the first region and dilatant fluid behavior in the second region. In the first region, the Power Law model was determined as the most suitable model for experimental data. In the second region, the Herschel-Bulkley model was found to be the most suitable model that was determined by statistical analysis.*

Keywords: *Fumed silica, polyethylene glycol, shear thickening fluid, non-Newtonian models.*

1. Introduction

Shear thickening fluid (STF) is a type of non-Newtonian fluid. In the shear thickening phenomenon, after the shear rate reaches a critical point, the viscosity of a fluid significantly increases. Different theories were proposed to explain these properties of shear thickening fluids. Order-Disorder Transition and Hydro-Cluster Theory are the most used of these theories [1–3].

In the early researches, the viscosity mechanisms of STFs were examined and parameters that affect these mechanisms were tried to determine. The effects of particle shapes [4], particle hardness [5], polyethylene glycol [6], and temperature [7] on shear thickening behavior have been investigated in various studies. In the literature, PEG [8,9] and EG [10,11], were used as a liquid medium, spherical [12] and fumed silica [13,14] as solid particles in STFs produced using a wide variety of suspensions.

In a study in the literature, the shear behavior of low molecular weight polyethylene glycol and silica suspensions were investigated. In rheological measurements, it was observed that fumed silica particles formed immobile aggregates in polyethylene glycol. Fumed silica, an amorphous silicon dioxide, consists of nano-sized, non-porous spherical particles branched aggregates. This system showed a complex steady shear behavior; shear-thickening between two shear-thinning regions. Shear-thinning behavior was observed in suspension that consists of polyethylene glycol of low molecular weight [15].

In an emulsion application in literature, the development and characterization processes of a continuous phase with fumed silica and surfactant were carried out. Ecological continuous phases were developed with the help of a green surfactant and fumed silica. A significant increase in viscoelastic flow was detected for the fumed silica-water system. This rheological change is related to the interaction of silica chains, as seen in the SEM images. As a result of the microstructure and the proposed properties, an increase in the physical stability of more concentrated systems was observed. It was determined that the viscoelastic properties related to the interaction between silica chains increase [16].

In another study with silica particles, size characterization was made by Sedimentation Field Flow when used as a food additive. There are four types of silica particles found as additives in food and personal care products. Dimensional characterization was made using analyzes such as SEM and TEM. Nanoparticle sizes of some samples organized into clusters or aggregates were determined by different analytical techniques. Along with the SEM observations, the added silicon oxide particles were identified and the particle size distribution was verified [17].

In the literature, the rheology of shear thickening of fumed silica and polyethylene glycol was investigated with nano-clay additive. The shear thickening properties of the mixture prepared in different concentrations, a modified clay, and fumed silica-polyethylene glycol were determined. The change in rheological properties of the mixture was studied when fumed silica or nano-clay was used in equal weight in polyethylene glycol. In the case of nano-clay addition at a temperature of 298 K, the increase in critical viscosity is less than that observed for the same amount of fumed silica. According to the rheological results, the elasticity and thermal stability of the mixture increased significantly with the addition of nano additives [18].

Shear thickening fluids are used in many fields due to their unique properties mentioned above. Personal body armor [19–21], protective clothing [8,22,23], and their use as vibration dampers [24,25] are the most common uses of these fluids. Yarn pull-out, surface friction, impact, and ballistic test of STF impregnated high-performance fabrics will be our future studies. Commercial use of these fabrics has become widespread in the defense industry. Increasing the energy absorption efficiency of the mentioned fabrics is commercially important.

Many studies were done to explain the effectiveness of these smart fluids in energy absorption. In this study, the comparison of rheological measurements of different molecular weight polyethylene glycols and fumed silica mixtures were made. By examining the non-Newtonian models, it was tried to decide the model suitable for the rheological results of the suspension produced. It is thought that

determining the non-Newtonian model of the produced mixtures will be effective in explaining the role of these fluids in energy absorption.

2. Materials and Methods

This study is to determine the most appropriate rheological model for shear thickening fluids produced using polyethylene glycols with different molecular weights. The rheological behavior of the STFs obtained by keeping constant the production method, the solid particles, and the concentration of suspension was examined. Fumed silica (Aerosil 200) which has a particle size of 12 nm and a specific surface area of 200 m^2/g was used as the solid particle in the production of STFs. Three different polyethylene glycols (PEGs) with different molar mass were used as the solvent. The average molar mass of PEGs used in this study was selected as 200, 300, and 400 g/mol. The physical and chemical properties of the polyethylene glycols and silica nanoparticles used as shown in Table 1 and Table 2.

Table 1. Properties of PEGs

Properties	PEG 200	PEG 300	PEG 400
Molecular weight (g/mol)	200	300	400
Density (kg/m^3)	1.1238	1.1250	1.1300
Flash temperature (℃)	150	220	305

Table 2. Properties of silica nanoparticle

Properties	Aerosil 200
Surface area (m^2/g)	200
Particle diameter (nm)	12
Tamped density (kg/m^3)	50
SiO_2 content (%)	99.8

Polyethylene glycols and silica particles were mixed with a high-speed mechanical mixer at 6000 rpm during the production of STFs. Silica particles were gradually added to prevent agglomeration and mixed until the suspension became homogeneous. The amount of fumed silica particles in the suspension was 25%(w/w).

Rheological properties of STFs were determined using Anton Paar MCR 102 tension controlled rheometer. Tests were carried out using a 25 mm diameter parallel plate apparatus. The gap between the plates was kept constant at 0.3 mm and all tests were performed at 25 ℃. Rheological measurements were made of 0-1000 s^{-1} shear rates. In the mixture, while shear-thinning behavior was observed at low shear rates, shear thickening was observed at high shear rates. In general, these mixtures exhibited the behavior of shear thinning between 0-200 s^{-1} and shear thickening between 200-1000 s^{-1} shear rates. The experimental parameters followed in the research are shown in Table 3.

Table 3. Experimental parameters

Sample	Temperature (K)	Time (hours)	Mixing Speed (rpm)	Aerosil	PEGs
1	298	-	-	-	200
2	298	1	6000	200	200
3	298	1	6000	200	300
4	298	1	6000	200	400

Table 4. Rheological model equations

No	Models	Equations
1	Power law	$\tau = \kappa \cdot (\dot{\gamma})^n$
2	Bingham	$\tau = \tau_0 + \kappa \cdot \dot{\gamma}$
3	Casson	$\tau^{0.5} = \tau_0 + \kappa \cdot \dot{\gamma}^{0.5}$
4	Herschel-Bulkley	$\tau = \tau_0 + \kappa \cdot \dot{\gamma}^n$
5	Sisko	$\tau = \kappa_\infty \cdot \dot{\gamma} + \kappa \cdot \dot{\gamma}^n$

The Non-Newtonian model equations used in the study given in Table 4. Correlation coefficients of theoretical equations in Table 5 and statistical error functions in Table 6 were analyzed and the most appropriate model equations were determined.

Table 5. Correlation coefficients for fumed silica-PEG mixtures in the first and second region at 298 K

Exp	Model	First Region				Second Region			
		n	κ	τ_0	κ_∞	n	κ	τ_0	κ_∞
1	1	0.99603	0.55967			0.99381	0.05621		
	2		0.05497	-0.0164			0.05371	0.17591	
	3		0.23450	-0.0035			0.23121	0.02931	
	4	0.98263	0.06033	-0.0569		1.04198	0.03936	1.39054	
	5	-0.0604	-0.0185		0.05495	0.89655	0.00625		0.05080
2	1	0.71471	6.68161			1.10787	18.5767		
	2		1.40504	25.9932			45.0013	-4814.7	
	3		1.00378	3.13339			7.05974	-24.101	
	4	0.75561	5.28216	6.66720		0.00001	$3.14\cdot10^9$	$-3.1\cdot10^9$	
	5	0.54776	8.59815		0.70092	-29.025	6.55876		37.8124
3	1	0.67095	12.3609			1.10693	27.8202		
	2		2.05292	43.4444			64.9175	-5784.3	
	3		1.18513	4.28628			8.48633	-26.051	
	4	0.67320	12.2001	0.61131		0.00006	$5.70\cdot10^8$	$-5.7\cdot10^8$	
	5	0.77710	11.5665		-1.4006	-43.856	10.4237		56.2807
	1	0.51375	32.6211			0.75771	325.867		
	2		2.98760	73.4298			54.1392	8191.11	
	3		1.27240	6.27467			6.42013	45.4158	
	4	0.50149	34.8680	-4.1584		0.35619	9118.50	-46340	
	5	0.47222	34.6863		0.44050	-52.208	12.1758		66.3696

Root mean square error (RMSE), Chi-square ($\square^2$), residual sum of squares (SSR), error sum of squares (SSE), sum of squares (SST) and R-squared are statistical parameters. In order to investigate the reliability of the results, the most appropriate model was determined by applying statistical tests such as RMSE and Chi-square in the equations. In Table 6, the most suitable model equations were determined by statistical analysis.

Table 6. Statistical analysis for fumed silica-PEG mixtures in the first and second region

Exp	Model	First Region				Second Region			
		R^2	RMSE	SSE	$\square^2$	R^2	RMSE	SSE	$\square^2$
	1	0.99875	0.13729	0.13193	0.04398	0.99967	0.24562	0.42230	0.14077
	2	0.99877	0.13709	0.13155	0.04385	0.99967	0.24629	0.42460	0.14153
	3	0.99876	0.13750	0.13234	0.04411	0.99967	0.24598	0.42353	0.14118

1	4	0.99881	0.13481	0.12722	0.04241	0.99958	0.27639	0.53473	0.17824
	5	0.99877	0.13708	0.13153	0.04384	0.99967	0.24561	0.42227	0.14076
2	1	0.99791	4.58217	146.974	48.9914	0.86263	4456.45	1.39×10^8	4.63×10^7
	2	0.98922	10.4050	757.853	252.618	0.88312	4110.84	1.18×10^8	3.94×10^7
	3	0.99719	5.31310	197.603	65.8677	0.87038	4329.07	1.31×10^8	4.37×10^7
	4	0.99852	3.85050	103.784	34.5947	0.97611	1954.75	2.68×10^7	8.92×10^6
	5	0.99823	4.21485	124.355	41.4516	0.85599	4562.98	1.46×10^8	4.86×10^7
3	1	0.99891	4.85223	164.809	54.9364	0.93150	4389.34	1.35×10^8	1.50×10^7
	2	0.97982	20.8963	3056.60	1018.87	0.94462	3946.71	1.09×10^8	3.64×10^7
	3	0.99377	11.6118	943.830	314.610	0.93691	4212.50	1.24×10^8	4.14×10^7
	4	0.99891	4.84813	164.531	54.8435	0.99764	814.909	4.65×10^6	1.55×10^6
	5	0.99909	4.44115	138.067	46.0222	0.92450	4608.38	1.49×10^8	4.96×10^7
4	1	0.98645	11.9746	1003.73	334.578	0.95106	3116.68	6.80×10^7	2.27×10^7
	2	0.93399	26.4341	4891.34	1630.45	0.93098	3701.28	9.59×10^7	3.20×10^7
	3	0.97189	17.2508	2083.14	694.380	0.94131	3413.05	8.15×10^7	2.72×10^7
	4	0.98652	11.9459	998.937	332.979	0.97994	1995.69	2.79×10^7	9.29×10^6
	5	0.98669	11.8707	986.393	328.798	0.87380	5005.06	1.75×10^8	5.85×10^7

3. Results and Discussion

It is seen in Figure 1 PEG 200 showed Newtonian behavior. In the first region, all Fumed silica-PEG suspensions to the critical shear rate showed shear-thinning behavior, and then in the second region shear thickening behavior was seen. In all suspensions increase of molecular mass of polyethylene glycol used as a liquid medium cause higher viscosity of the mixture. Critical shear rate is an important parameter for solidation. This value defines the line between solid and liquid medium. Increasing PEG's molecular mass causes decreasing in critical shear rate.

In Figure 2, the relation between the shear rate and the shear stress of the fumed silica-PEGs mixtures was investigated. While non-Newtonian properties are observed in the mixtures, Newtonian properties are also observed in polyethylene glycol 200.
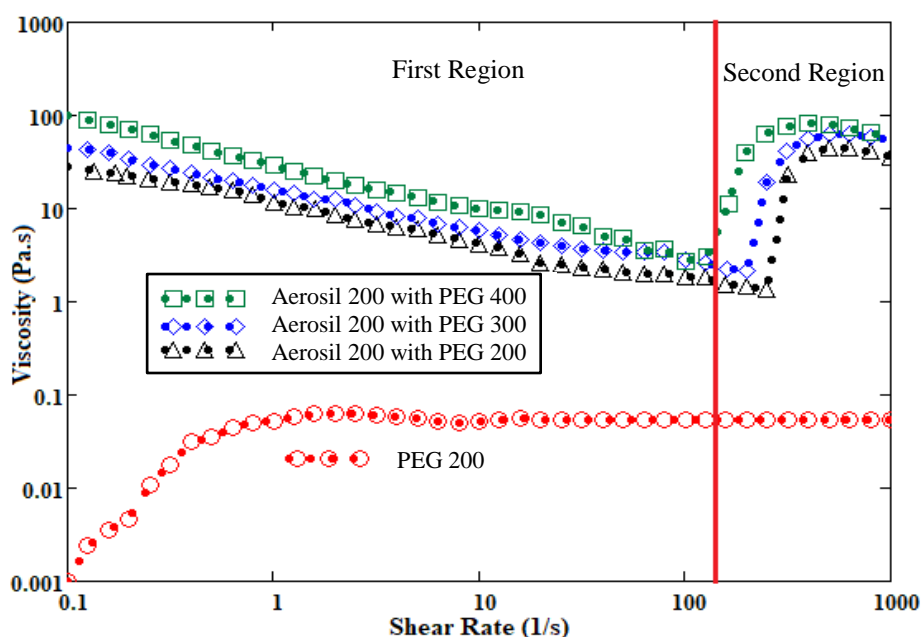

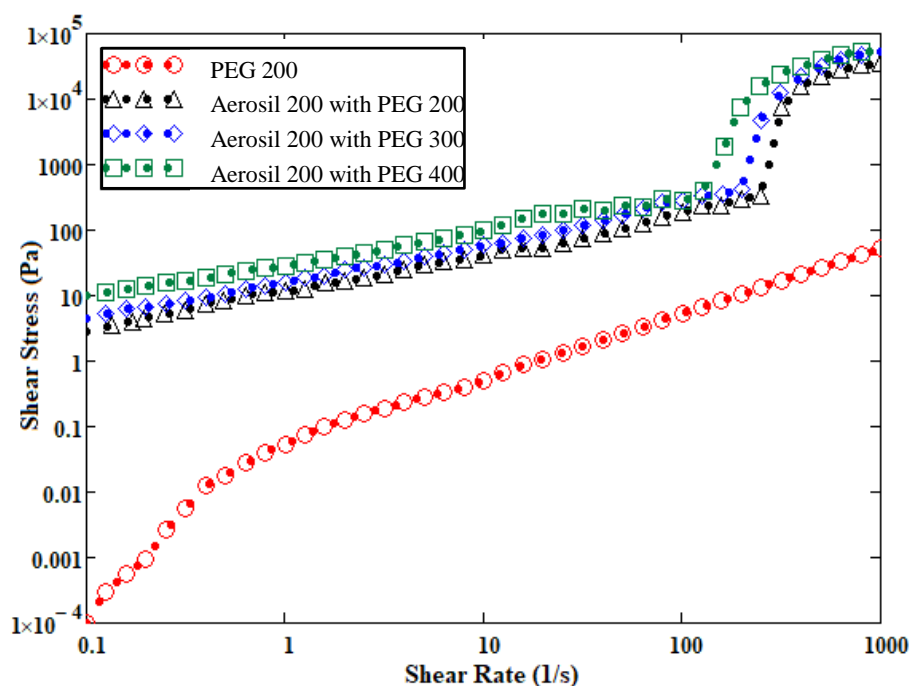**Figure 1.** Change of viscosity with different shear rate for fumed silica-PEG mixtures

Figure 2. Change of shear stress with the different shear rate for fumed silica-PEG mixtures

In the FTIR spectrum in Fig. 4; 3450 cm^{-1} O-H stretching vibrations, 2950 cm^{-1} C-H stretching vibrations, and 1550 cm^{-1} C=O stretching vibrations. It also shows 1150 cm^{-1} C-O stretching vibrations, 1050 cm^{-1} Si-O-Si stretching vibrations, and 850 cm^{-1} Si-O stretching vibrations. FTIR spectrum of the samples was made with Shimadzu S11025C device.
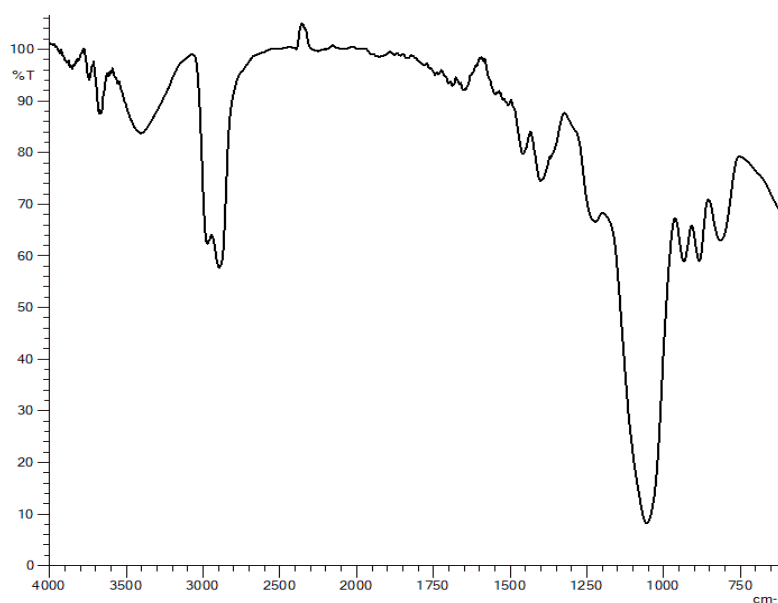

Figure 3. FTIR Spectrum for the mixture of Aerosil 200 and polyethylene glycol 200

4. Conclusions

In this study, fumed silica was dispersed in polyethylene glycol in colloidal structure. Physical attraction forces formed between them enabled the formation of shear thickening fluid by providing interaction between molecules. Three different PEGs were used to determine the effect of different PEGs in suspensions. The rheological behaviors of the suspensions produced were determined. It was observed

that as the molecular weight increases, the critical shear rate decreases, and the viscosity increases. The experimental data and theoretical models were compared by statistical analysis. The most appropriate model was selected by determining the error functions and correlation coefficients. For fumed silica-PEG mixtures that have different rheological behavior in the first and second regions, the model equations are calculated separately. In order to investigate the reliability of the results obtained from the models, the values in which root mean square error (RMSE), Chi-square (X^2), residual sum of squares (SSR), error sum of squares (SSE), and the total sum of squares (SST) errors are minimum if R-squared (SST) errors are examined in these models. These statistical models were compared to have more accurate results. Fumed silica-PEG mixtures showed pseudo-plastic behavior in the first region and dilatant liquid behavior in the second region. In the first region, the Sisko model was determined as the most appropriate model for experimental data. In the second region, the Herschel-Bulkley model was found to be the most appropriate model.

The compliance to the Research and Publication Ethics: This study was carried out in accordance with the rules of research and publication ethics.

References

[1] Hoffman R. L.,"Discontinuous and dilatant viscosity behavior in concentrated suspensions. II. Theory and experimental tests", *J. Colloid Interface Sci.*, 46(3), 491-506, 1974.

[2] Bossis G. and Brady J. F., "The rheology of Brownian suspensions," *J. Chem. Phys.*, 91(3), 1866-1874, 1989.

[3] Boersma W. H., Laven J., and Stein H. N., "Viscoelastic properties of concentrated shear-thickening dispersions," *J. Colloid Interface Sci.*, 149(1), 10-22, 1992.

[4] Lee B. W., Kim I. J., and Kim C. G., "The influence of the particle size of silica on the ballistic performance of fabrics impregnated with silica colloidal suspension," *J. Compos. Mater.*, 43(23), 2679-2698, 2009.

[5] Kalman D. P., Merrill R. L., Wagner N. J., and Wetzel E. D., "Effect of particle hardness on the penetration behavior of fabrics intercalated with dry particles and concentrated particle-fluid suspensions," *ACS Appl. Mater. Interfaces*, 1(11), 2602-2012, 2009.

[6] Baharvandi H. R., Alebooyeh M., Alizadeh M., Heydari M. S., Kordani N. and Khaksari P., "The influences of particle–particle interaction and viscosity of carrier fluid on characteristics of silica and calcium carbonate suspensions-coated Twaron® composite," *J. Exp. Nanosci.*, 11(7), 550–563, 2016.

[7] Hasanzadeh M., V. Mottaghitalab, and M. Rezaei, "Rheological and viscoelastic behavior of concentrated colloidal suspensions of silica nanoparticles: A response surface methodology approach," *Adv. Powder Technol.*, 26(6), 1570–1577, 2015.

[8] Gürgen S., "An investigation on composite laminates including shear thickening fluid under stab condition," *J. Compos. Mater.*, 53(8), 1111–1122, 2019.

[9] Xu Y., "Stabbing Resistance of Soft Ballistic Body Armour Impregnated with Shear Thickening Fluid," Ph. D. thesis, University of Manchester, Manchester, UK, 2016.

[10] Chen Q., Liu M., Xuan S., Jiang W., Cao S., and Gong X., "Shear dependent electrical property of conductive shear thickening fluid," *Mater. Des.*, 121, 92–100, 2017.

[11] Sun L. L., Xiong D. S., and Xu C. Y., "Application of shear thickening fluid in ultra high molecular weight polyethylene fabric," *J. Appl. Polym. Sci.*, 129(4), 1922–1928, 2013.

[12] Ge J., Tan Z., Li W. and Zhang H., "The rheological properties of shear thickening fluid reinforced with SiC nanowires," *Results Phys.*, 7, 3369–3372, 2017.

[13] Hasanzadeh M. and Mottaghitalab V., "Tuning of the rheological properties of concentrated silica suspensions using carbon nanotubes," *Rheol. Acta*, 55(9), 759–766, 2016.

[14] Zabet M., Trinh K., Toghiani H., Lacy T. E., Pittman C. U., and Kundu S., "Anisotropic Nanoparticles Contributing to Shear-Thickening Behavior of Fumed Silica Suspensions," *ACS Omega*, 2(12), 8877–8887, 2017.

[15] Rubio-Hernández F. J., Gómez-Merino A. I., Páez-Flor N. M., and Velázquez-Navarro J. F., "On the steady shear behavior of hydrophobic fumed silica suspensions in PPG and PEG of low molecular weight," *Soft Materials*, 15(1), 55-63, 2017.

[16] Santos J., Calero N., Trujillo-Cayado L. A. and Muñoz J., "Development and characterisation of a continuous phase based on a fumed silica and a green surfactant with emulsion applications," *Colloids Surfaces A Physicochem. Engineering Aspects*, 555(20), 351-357, 2018.

[17] Contado C., Ravani L. and Passarella M., "Size characterization by Sedimentation Field Flow Fractionation of silica particles used as food additives," *Anal. Chim. Acta*, 788, 183-192, 2013.

[18] Singh M., Verma S. K., Biswas I. and Mehta R., "Rheology of fumed silica and polyethylene glycol shear thickening suspension with nano-clay as an additive," *Def. Sci. J.*, 69(4), 402-408, 2019.

[19] Mawkhlieng U. and Majumdar A., "Designing of hybrid soft body armour using high-performance unidirectional and woven fabrics impregnated with shear thickening fluid," *Compos. Struct.*, 253, 2020.

[20] Majumdar A.,. Laha A, Bhattacharjee D., Biswas I. and Verma S., "Soft body armour development by silica particle based shear thickening fluid coated p-aramid fabrics," *J. Text. Inst.*, 110(10), 1515–1518, 2019.

[21]   Arora S., Majumdar A. and Butola B. S., "Soft armour design by angular stacking of shear thickening fluid impregnated high-performance fabrics for quasi-isotropic ballistic response," *Compos. Struct.*, 233, 2020.

[22] Li T. T., Cen X., Peng H., Ren H., Han L., Lou C.W. and Lin J.H., "Rheological response and quasi-static stab resistance of STF/MWCNTs-impregnated aramid fabrics with different textures," *J. Ind. Text.*, 50(3), 380–397, 2020.

[23]Zarei M. and Aalaie J., "Application of shear thickening fluids in material development," *J. Mater. Res. Technol.*, 9(5), 10411–10433, 2020.

[24]Lin K., Zhou A., Liu H., Liu Y. and Huang C., "Shear thickening fluid damper and its application to vibration mitigation of stay cable," *Structures*, 26, 214–223, 2020.

[25]Gürgen S. and Sofuoğlu M. A., "Vibration attenuation of sandwich structures filled with shear thickening fluids," *Compos. Part B Eng.*, 186, 2020.

INESEG
INTERNATIONAL
ENGINEERING,
SCIENCE AND
EDUCATION GROUP

MEJS

Research Article

ESSENTIAL ELEMENTS AND HEAVY METAL LEVELS IN SHEEP MILK AND ITS DAIRY PRODUCTS

Serap KILIÇ ALTUN[1]* ⓘ *Mehmet Emin AYDEMİR[1]* ⓘ
[1]*Harran University, Veterinary Faculty, Department of Food Hygiene and Technology, Şanlıurfa, Turkey
* Corresponding author; skilicaltun@harran.edu.tr

Abstract: *Milk and various dairy products are among the basic foods used in nutrition. However, milk and dairy products can contain many environmental pollutants such as pesticides, detergents, drug residues, heavy metals that may pose technological risks and are dangerous for human health. The aim of this study is to reveal the change of the amounts of essential elements and heavy metals in sheep's milk, yoghurt, buttermilk, and butter which are produced from the same milk. For this purpose, yoghurt, buttermilk, and butter were made from sheep's milk. Then, in milk and dairy products, Sodium (Na), Magnesium (Mg), Potassium (K), Manganese (Mn), Copper (Cu), Zinc (Zn), Arsenic (As), Selenium (Se)), Cadmium (Cd), Lead (Pb) amounts were examined by ICP-MS. The amount of As, Cd, Pb in all samples were determined under the limit of detection (LOD). The amounts of Na, Mg, K, Mn, Cu, Zn, Se in milk were determined as 785, 92, 1537, 30,8, 73,5, 2683,5, 381,5 ppb, respectively. The amounts of Na, Mg, K, Mn, Cu, Zn, Se in yogurt were determined as 554,5, 121,5, 1516,5, 29,3, 71,5, 3692, 405 ppb, respectively. The amounts of Na, Mg, K, Mn, Cu, Zn, and Se in buttermilk were determined as 40175, 56,5, 553,5, 111,5, 1230, 2506,5, 447 ppb, respectively. The amounts of Na, Mg, K, Mn, Cu, Zn, Se in butter were determined as 98,2, 31,7, 223,1, 10,1, 24,6, 203,5, 282,5 ppb, respectively. According to these data, changes in the amount of essential elements were observed when milk was transformed into its products. It was determined that there were no heavy metals in sheep milk and products grown in this region.*

Keywords: *Sheep milk, Dairy product, Element, Heavy metal, ICP-MS*

Received: October 14, 2020   Accepted: December 22, 2020

1.Introduction

Milk is produced in the milk glands of female mammals to feed their offspring. Various foods derived from milk are called "dairy products" such as cheese, cream, yoghurt, buttermilk, butter [1]. Milk and dairy products are among the basic foods used in human nutrition. Milk and dairy products are among the foods that are highly preferred by consumers because they have high biological values rich in nutrients, are thought to have little health risk, and are especially easily accessible. However, milk and dairy products may contain many environmental pollutants such as pesticides, detergents, drug residues, heavy metals that may pose technological risks and are dangerous for human health [2].

The heavy metal term is a general nomenclature given to heavy metals with an atomic number greater than 20 or a volume occupying one cubic centimeter more than five grams [3]. Heavy metals tend to accumulate in the tissues of the mammalian body, reaching toxic values over time and may cause serious health problems [4]. Heavy metals enter the human body through digestion, respiration, and skin. Acute, subacute and chronic intoxication symptoms (such as microcytic anemia, liver necrosis, memory retardation, speech, and voice disorders) occur depending on overdose, frequency, and duration of intake [5].

The level of elements found in milk and dairy products is very important due to their essential or toxic effects. For example, although Cd, As, Pb are toxic, Cu, Se Zn, Cr, Na, Mg, Mn are essential and are toxic only at high doses. Among the elements that have negative effects on human health, Pb, As and Cd are the most dangerous [6, 7]. Considering that milk and dairy products are one of the basic foods, the possibility of having high amounts of lead, cadmium, copper, and zinc residues in milk poses a serious risk. Children are more sensitive to heavy metals than adults. Because heavy metals accumulate in the tissues and very small amounts of milk can cause serious effects on the health of children. For example, slowing down in mental development, decrease in concentration can negatively affect kidney and heart health [8, 9].

Heavy metal contamination of milk and dairy products; The feed consumed by the animals from which milk is obtained can pass directly to the milk as a result of contamination with the animal through the water they drink and the air they breathe [10]. In addition, contamination can occur from machinery and equipment that come into contact with dairy products during the production and storage of milk and dairy products. Contamination may occur during technological processes or from metal containers and operational water used to preserve milk and milk products. Even if there is no heavy metal contamination in the milk to be used in technology, heavy metal can be detected after milk is processed (cheese, yogurt, buttermilk, butter). This is the result of metals in the composition of containers used in the production of acidic dairy products, dissolving into the product. The main elements in water and metallic contamination used in the business are copper, zinc, iron, tin, lead, arsenic, and cadmium [11, 12].

Akin et al. (2003) reported that the high level of aluminum they detected in raw milk may be caused by tools and equipment made of aluminum metal in addition to the feed consumed by animals [13]. Yuzbasi (2001) found that the amount of lead in the milk to be processed into cheddar cheese decreased significantly in cheddar cheeses after production, there was no change in the amount of copper, but the amount of cadmium increased [10]. Temurci and Güner. (2006) reported that when they examined heavy metal levels in milk and cheese obtained from these milks, they found that aluminum, chromium, copper, and iron amounts in cheese samples were higher than milk samples [14]. In this study, we aimed to demonstrate the change of essential element and heavy metal amounts in sheep's milk, yoghurt, buttermilk, and butter that we produce from this milk with the ICP-MS device.

2. Material Method

In this study, samples of milk belonging to ivesi breed sheep taken from the farm of Harran University, and samples of yoghurt, buttermilk, and butter produced from this milk formed the material of the study (Figure 1-3) [15].
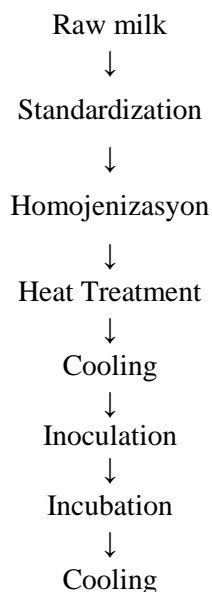
Raw milk
↓
Standardization
↓
Homojenizasyon
↓
Heat Treatment
↓
Cooling
↓
Inoculation
↓
Incubation
↓
Cooling

Figure 1. Yoghurt production stages

Yoghurt
↓
Addition of water
(50:50 v/v)
↓
Addition of salt
(c.a. 0.5%)
↓
Mixing
↓
Buttermilk

Figure 2. Buttermilk production stages

Yoghurt
↓
Addition of water
(70:30 v/v)
↓
Churning (10 ^{0}C)
↓
Washing

Figure 3. Butter production stages

After dairy products are prepared in the laboratory, 1 gram of milk, cheese, yoghurt, and butter samples were weighed after the homogenization process and taken into the sample containers of the microwave device. 4 mL of 65% (v / v) nitric acid (HNO3) and 2 mL of 30% (v / v) hydrogen peroxide (H2O2) were added with a pipette and placed in the microwave device. The samples were burned in the microwave device with the predetermined program (Table 1). After burning the samples cooled, they were taken into sterile tubes and diluted with ultrapure water.

Table 1. Burning process steps in microwave device

Step	Temperature (ºC)	Time (min)
1	90	8
2	170	10
3	210	25

Elemental and heavy metal analyzes of the samples were performed with the Agilent brand, 7500ce series ICP-MS (Tokyo, Japan) device in the Mersin University Advanced Technology Education, Research and Application Center laboratory.

3. Results and Discussion

In this study, the element and heavy metal amount of each sample analyzed by ICP-MS is shown in Table 2. and Figure 4.
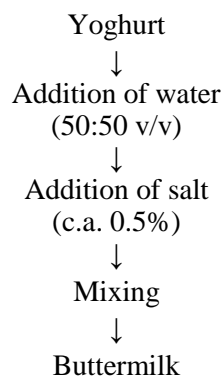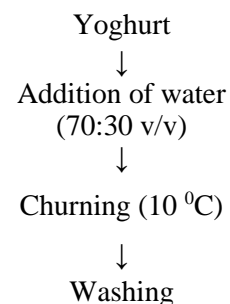
Table 2. The element and heavy metal content of sheep milk and its dairy products

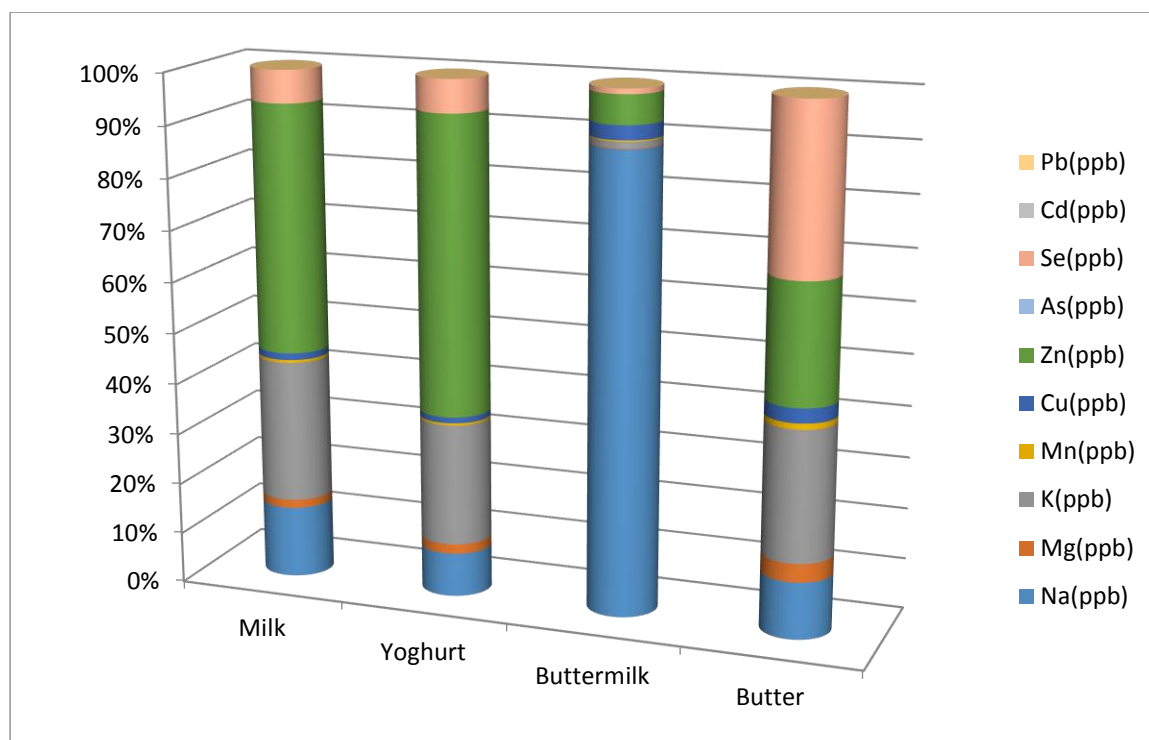| Element	Milk	Yoghurt	Buttermilk	Butter
Na (ppb)	785	554.5	40175	98.2
Mg (ppb)	92	121.5	56.5	31.7
K (ppb)	1537	1516.5	553.5	223.1
Mn (ppb)	30.8	29.3	111.5	10.1
Cu (ppb)	73.5	71.5	1230	24.6
Zn (ppb)	2683.5	3692	2506.5	203.5
As (ppb)	<LOD	<LOD	<LOD	<LOD
Se (ppb)	381.5	405	447	282.5
Cd (ppb)	<LOD	<LOD	<LOD	<LOD
Pb (ppb)	<LOD	<LOD	<LOD	<LOD

Figure 4. The element and heavy metal content of sheep milk and its dairy products

Micronutrients such as copper, magnesium, potassium, and zinc are essential for many biological functions. The deficiencies of such elements in the body contribute significantly to the emergence of many diseases. However, if these elements are found in foods at higher levels, they can have negative effects on human health [16]. The trace element content and heavy metal contents of milk and dairy products may vary depending on the lactation stage, the nutritional status of the animal, environmental and genetic factors, and possible contamination during production [17]. In this study we conducted, firstly, the mineral and heavy metal amounts in milk and then in dairy products produced from that milk were examined. There was a change in the amount of minerals seen (yoghurt, buttermilk, butter) (Table 2, Figüre 4.).

Na has many beneficial effects in the body, such as osmotic pressure, electrolyte balance, acid-base balance, and electrochemical impulse transmission across nerve and muscle membranes [18]. There is also some Na in milk and dairy products. However, the amount of Na in milk and dairy products varies according to the lactation period, nutritional status and the process applied to the milk. In a study conducted by Güler (2007), heavy metal analyzes were made on yoghurts produced from goat milk and goat milk collected from Hatay. Na levels were determined as 433 ppm for raw milk, 520 ppm for strained yogurt, and 5147 ppm for salted strained yogurt, respectively [19]. In our study, the amount of Na was 785 ppb in milk, 554,5 ppb in yogurt, 40 175 ppb in buttermilk, and 98,2 ppb in butter. Na amount was determined in the highest buttermilk. The reason for the high amount of Na in buttermilk is due to the addition of NaCl during construction.

Mg has many functions involved in more than 300 reactions in the body. Mg is found in most foods. It is a good source of Mg in milk and dairy products. There is about 100 mg of Mg in one liter [20]. The amount of Mg varies according to the lactation period, the animal's diet and the process applied

to the milk. In a study conducted by Güler (2007), heavy metal analyzes were made on yoghurts produced from goat milk and goat milk collected from Hatay. Mg levels were determined as 510 ppm for raw milk, 587 ppm for strained yogurt, and 838 ppm for salted strained yogurt, respectively [19]. In our study, the amount of Mg was 92 ppb in milk, 121,5 ppb in yoghurt made from milk, 56,5 ppb in buttermilk, and 31,7 ppb in butter. The amount of Mg was found the most in yogurt and the least in butter.

K has many beneficial effects osmotic pressure, electrolyte balance, acid-base balance, nerve impulses, contraction of the heart and other muscles, protein synthesis, conversion of glucose into glycogen in the body [18]. Therefore, K should be taken from outside with food. The amount of K changes according to the lactation period, the animal's diet and the process applied to the milk. In a study conducted by Güler (2007), heavy metal analyzes were made on yoghurts produced from goat milk and goat milk collected from Hatay. K levels were determined as 409 ppm for raw milk, 511 ppm for strained yogurt, and 554 ppm for salted strained yogurt, respectively [19]. In our study, the amount of K was 1537 ppb in milk, 1516,5 ppb in yoghurt made from milk, 553,5 ppb in buttermilk, and 223,1 ppb in butter. K amount was determined mostly in yoghurt. The low amount of K element in butter and buttermilk suggests that it may be due to the production process.

Mn participates in cofactor, reproduction, and bone structure in many enzymatic reactions in the body and is necessary because it has many functions such as regulating brain functions. Therefore, Mn should be taken from outside with food [18]. It contains some Mn element in milk and dairy products. The amount of Mn varies according to the lactation period, the animal's feeding, and the process applied to the milk. Enb et al. (2009), in their study with buffalo and cow milk, determined the amount of Mn in buffalo milk as 0.076 mg/kg and the amount of Mn in cow milk as 0.056 mg/kg. In the same study, the highest amount of Mn in dairy products such as cream and butter was determined as 0.316 mg/kg in butter and 0.234 mg/kg in cream [21]. Kaya et al. (2008) reported metal concentrations in yoghurt made from cow's milk in a controlled environment as 0.01-0.179 mg/kg for Mn [22]. In our study, the amount of Mn was 30,8 ppb in milk, 29,3 ppb in yoghurt made from milk, 11,5 ppb in buttermilk, and 10.1 ppb in butter. While Mn amounts were higher in milk and yoghurt, the amount of Mn in buttermilk and butter decreased.

Cu is required as a trace element necessary for adequate growth, cardiovascular system, lungs, neuronendocrine function, and iron metabolism [23] Excess Cu taken into the body due to contamination or other reasons may cause poisoning effect and cause hypercoupremia. Generally, the Cu level contained in milk is at minimum levels but With subsequent contamination, Cu in milk and dairy products can be seen at maximum level [24]. Kaya et al. (2008) reported metal concentrations in yogurt made from cow's milk in a controlled environment as 0.011-0.498 mg / kg for Cu [22]. Temurci and Güner. (2006) reported that when they examined heavy metal levels in milk and cheese obtained from these milks, the amount of Cu in cheese samples was higher than in milk samples [14]. Yuzbasi (2001) reported that the amount of Cu in milk to be processed into cheddar cheese does not change in cheddar cheese after production [10]. Gördes Baş (2020) reported that the Cu amount in yoghurt and buttermilk offered for consumption was 0.03 mg/kg in yoghurt and 0.01 mg/kg in buttermilk [25]. In a study conducted by Kan and Küçükkurt (2018), Cu amount was reported as 0.09 mg/kg in cream and 0.02 mg / L in cream milk [26]. In this study we conducted, Cu amount was 73,5 ppb in milk, 71,5 ppb in yoghurt made from milk, 1230 ppb in buttermilk, and 24,6 ppb in butter. The high amount of Cu in buttermilk

is thought to be due to the use of metal containers in the production of buttermilk and adding water from the outside. The probable reason for the high Cu content in buttermilk is due to the added salt or water.

Zn is involved in many physiological processes such as nucleic acid and protein synthesis, cellular replication, insulin secretion, sexual maturation, and strengthening of the immune system [27]. Enb et al. (2009) found the Zn value in milk as 4,350 mg / kg, in yogurt 4,059 mg / kg, in cream 19,570 mg / kg and in butter 29,363 mg / kg in their heavy metal analysis by collecting milk from buffalo and cow milk and obtaining dairy products [21]. Gördes Baş (2020) reported that the amount of Zn in yoghurt and buttermilk offered for consumption is 3.05 mg / kg in yoghurt and 1.66 mg / kg in buttermilk [25]. In a study conducted by Güler (2007), heavy metal analyzes were made on yoghurts produced from goat milk and goat milk collected from Hatay. Zn levels were determined as 4.68 ppm for raw milk, 6.85 ppm for strained yogurt, and 9.00 ppm for salted strained yogurt, respectively [19]. In a study by Kan and Küçükkurt (2018), the amount of Zn was reported as 8.27 mg/kg in cream and 2.37mg / L in skim milk [26]. In this study, the amount of Zn was determined as 2683,5 ppb in milk, 3692 ppb in yogurt made from milk, 2506,5 ppb in buttermilk, and 203.5 ppb in butter. The Zn amount was found in the highest yogurt and the lowest in butter. As the Zn element attaches to the casein micelles in yoghurt production, it was detected at a higher rate in yoghurt.

Se plays an important role in immunity, antioxidant system, DNA synthesis, and DNA repair. The recommended daily intake of Se is 55 µg. It is an important source of Se in milk and dairy products [20]. Setting et al. (2007) investigated some heavy metals in various dairy products and found the highest Se value in Tulum cheese with 0.434 mg/kg and then in butter with 0.315 mg/kg [28]. In a study conducted by Güler (2007), heavy metal analyzes were made on yoghurts produced from goat milk and goat milk collected from Hatay. Se levels were determined as 7.59 ppm for raw milk, 10.77 ppm for strained yogurt, and 12.20 ppm for salted strained yogurt, respectively [19]. In a study by Kan and Küçükkurt (2018), the amount of Se was reported as 0.94 mg/kg in skim milk and 0.17 mg / L in skim milk [26]. In our study, the amount of Se was 381,5 ppb in milk, 405 ppb in yogurt made from milk, 447 ppb in buttermilk, and 282,5 ppb in butter.

The amounts of Se in all samples were determined at close levels.

Since heavy metals cause acute and chronic health problems, national and international food organizations have introduced regulations to prevent contamination. However, in the communiqué of the Turkish Food Codex on determining the maximum levels of certain contaminants in foodstuffs [29], the highest acceptable values for milk and dairy products were determined as 0.020 mg/kg for Pb, but no limit was specified for other metals. In this study, the amounts of Pb, As and Cd in milk, yoghurt, buttermilk, and butter were analyzed. These heavy metals were not detected in any of the samples in the analysis results.

The presence of Pb in milk and dairy products is from environmental sources (atmosphere, vehicle exhausts, urban waste, etc.). Since Pb is toxic and has negative effects on human health, the Codex Alimentarius Commission [30] determined the Pb amount at the level of 0.02 mg/kg for milk and dairy products. Also, The Turkish Food Codex states that the highest acceptable Pb for milk and dairy products is 0.020 mg/kg [29]. In a study conducted by Güler (2007), heavy metal analyzes were made on yoghurts produced from goat milk and goat milk collected from Hatay. Pb levels were determined as 0.06 ppm for raw milk, 0.11 ppm for strained yoghurt, and 1,3 ppm for salted strained yogurt, respectively [19]. Kaya et al. (2008) reported metal concentrations in yogurt made from cow's milk in a controlled environment as 0.019-0.126 mg/kg for Pb [22]. In a study conducted by Hernandez and Park

(2014), they reported the Pb amount of 3 different yoghurts made from goat milk obtained from a market as 4,003-4,280ppm [31]. Coni et al. (1999) in a study conducted in Italy; Pb amount is 0.006 ± 0.003 ppm in sheep milk, 0.016 ± 0.006 ppm in curd obtained from sheep milk, 0.003 ± 0.001 ppm in whey obtained from sheep's milk, 0.019 ± 0.006 ppm in Pecorino cheese obtained from sheep milk, 0.002 in Ricatta cheese obtained from sheep milk. It has been reported as ± 0.001 [32]. Yuzbasi (2001) reported that the amount of Pb in the milk to be processed into cheddar cheese decreased significantly in post-production cheddar cheese [10]. In a study by Kan and Küçükkurt (2018), it was reported that the amount of Pb shifts and the average values are the same in under-cream milk, while the standard deviation and maximum value are higher in under-cream milk [26]. Gördes Baş (2020) reported that he did not detect Pb in yoghurt and buttermilk offered for consumption [25]. In our study, the amount of Pb was found below the detection limits (<LOD) in milk and yoghurt made from milk, buttermilk, and butter.

Cd can contaminate milk and dairy products from the environment (soil, fertilizer, atmosphere). It is considered the most important food contaminant. Cd is important because it shows high toxicity and has negative effects on human health (8). Turkish Food Codex does not set any limit for Cd. In a study conducted by Güler (2007), heavy metal analyzes were made on yoghurts produced from goat milk and goat milk collected from Hatay. Cd levels were determined as 0.63 ppm for raw milk, 1.01 ppm for strained yoghurt, and 1.00 ppm for salted strained yogurt, respectively [19]. In a study conducted by Hernandez and Park (2014), they reported the Cd amount of 3 different yoghurts made from goat milk obtained from a supermarket as 0.614-0.700 ppm [31]. Coni et al. (1999) in a study conducted in Italy; The amount of Cd in sheep's milk is 0.058 ± 0.019 ppm. It has been reported as 0.048 ± 0.016 ppm in curd obtained from sheep milk, 0.076 ± 0.035 ppm in whey obtained from sheep milk, 0.025 ± 0.009 ppm in Pecorino cheese obtained from sheep milk, and 0.043 ± 0.013 ppm in Ricatta cheese obtained from sheep milk [32]. Yuzbasi (2001) reported that the amount of Cd in the milk to be processed into cheddar cheese increased in cheddar cheese after production [10]. In a study by Kan and Küçükkurt (2018), the amount of Cd in cream and cream milk was found below the detectable value [26]. Gördes Baş (2020) reported that he did not detect Pb in yoghurt and buttermilk offered for consumption [25]. In this study we conducted, the amount of Cd was found below the detection limits (<LOD) in milk and yoghurt, buttermilk and butter made from milk.

As it is common in nature and increasing exposure to environmental arsenic today, high arsenic content in some products has increased. As is also contaminated with milk and dairy products from the environment (1). In a study by Kan and Küçükkurt (2018), the amount of As was reported as 0.14 mg/kg in skim milk and 0.04mg / L in skim milk [26]. In a study conducted by Güler (2007), heavy metal analyzes were made on goat milk collected from Hatay and yoghurts produced from goat milk [19]. Arsenic has not been detected in any product. Gördes Baş (2020) reported that he did not detect As in yoghurt and buttermilk offered for consumption [25]. In our study, the amount of As was found below the detection limits (<LOD) in yoghurt, buttermilk, and butter made from milk and milk.

4. Conclusion

According to these data, changes in the amount of essential elements were observed when milk was transformed into its products. It was determined that there were no heavy metals in sheep milk and products grown in this area. This study shows that sheep's milk and products can contribute significantly to the supply of elements in the human diet. It also provides important information on essential elements

and heavy metal concentration about the safety and quality standards of sheep's milk, yoghurt, buttermilk, and butter.

The compliance to the Research and Publication Ethics: This study was carried out in accordance with the rules of research and publication ethics.

References

[1] İstanbulluoğlu, H., Oğur, R., Tekbaş, Ö. F., Bakır, B. "Süt ve süt ürünlerinde ağır metal kirliliği", *Türkiye Klinikleri Tıp Bilimleri Dergisi*, *33*(2), 410-419, 2013.

[2] Lıcata, P., Trombetta, D., Crıstanı, M., Gıofre, F., Martıno, D., Calo, M., Naccarı, F. "Levels of "toxic" and "essential" metals in samples of bovine milk from various dairy farms in Calabria", *Italy. Environ Int.* 30(1), 1-6, 2004.

[3] Agarwal, S.K., *Heavy Metal Pollution*. Vol: 4 APH Publishing, 2009.

[4] Hernández, A.J., Gutiérrez-Ginés, M.J., Pastor, J., *Ecology And Health İn Risk Analysis Of Polluted Soils. Environmental health risk.* WIT Press, Southampton, pp. 257-268, 2009.

[5] Kaya, S., Prinçci, İ., Bilgili, A., *Veteriner Hekimliğinde Toksikoloji*. Medisan Yayınevi, 2002.

[6] Liu, Z.P., "Lead poisoning combined with cadmium in sheep and horses in the vicinity of non-ferrous metal smelters", *The Science of the Total Environment*, 309, 117–126, 2003.

[7] Martino, F.A.R., Sánchez, M.L.F., Medel, A, S., "Total determination of essential and toxic elements in milk whey by double focusing ICP-MS", *Journal of Analytical Atomic Spectrometry*, 15, 163–168, 2000.

[8] Girma, K., Tilahun, Z., Haimanot, D., "Review on milk safety with emphasis on ıts public health", *World Journal of Dairy & Food Sciences,* 9(2), 166- 183, 2014.

[9] Hizel, S., Şanlı, C., "Çocuklarda beslenme ve kurşun etkileşimi", *Çocuk Sağlığı ve Hastalıkları Dergisi*, 49, 333- 338, 2006

[10] Yüzbaşı, N., Kaşar Peynirinde Bazı Ağır Metallerin Düzeyi ve Prosesteki Değişimi, Doktora Tezi, Ankara Üniversitesi Ankara, Türkiye, 2001.

[11] Metin M., *Süt Teknolojisi.* Ege Üniversitesi Basımevi, 2001.

[12] Pečar, D., Slemnik, M., Goršek, A., "Testing the corrosion resistance of stainless steels during the fermentation of probiotic drink", *J. Sci. Food Agric.,* 91(7), 1293-7, 2011.

[13] Akın, N., Ayar, A., Sert, D., Çalık, N., "Konya ilinin değişik bölgelerinden toplanan sütlerin ağır metal içerikleri üzerine bir araştırma" Süt Endüstrisinde Yeni Eğilimler Sempozyumu, İzmir, Türkiye, 2003, s. 355-358.

[14] Temurci, H., Güner, A., "Ankara'da tüketime sunulan süt ve beyaz peynirlerde ağır metal kontaminasyonu", *Atatürk Üniversitesi Veteriner Bilimleri Dergisi*, *1*(2), 20-28, 2006.

[15] Tekinsen, O.C., Tekinsen, K.K., *Süt ve Süt Urunleri : Temel Bilgiler, Teknoloji, Kalite Kontrolu.* Selcuk Universitesi Basimevi, 2005.

[16] Kazi, T.G., Jalbani, N., Baig, J.A., Kandhro, G.A., Afridi, H.I., Arain, M. B., Shah, A.Q., "Assessment of toxic metals in raw and processed milk samples using electrothermal atomic absorption spectrophotometer", *Food and Chemical Toxicology*, *47*(9), 2163-2169, 2009.

[17] Meshref, A.M., Moselhy, W.A., Hassan, N.E.H.Y., "Heavy metals and trace elements levels in milk and milk products", *Journal of food measurement and characterization*, *8*(4), 381-388, 2014.

[18] Özturan, K., Atasever, M., "Süt ve ürünlerinde mineral maddeler ve ağır metaller", *Atatürk Üniversitesi Veteriner Bilimleri Dergisi*, *13*(2), 229-241, 2018.

[19] Güler, Z., "Levels of 24 minerals in local goat milk, its strained yoghurt and salted yoghurt (tuzlu yoğurt", *Small Ruminant Research*, *71*(1-3), 130-137, 2007.

[20] Haug, A., Høstmark, A.T., Harstad, O.M., "Bovine milk in human nutrition–a review", *Lipids in health and disease*, *6*(1), 25, 2007.

[21] Enb, A., Abou Donia, M.A., Abd-Rabou, N.S., Abou-Arab, A.A.K., El-Senaity, M.H., "Chemical composition of raw milk and heavy metals bahavior during processing of milk products", *Global Veterinaria,* 3 (3): 268 – 275, 2009.

[22] Kaya, G., Akdeniz, I., Yaman, M., "Determination of Cu, Mn, and Pb in yogurt samples by flame atomic absorption spectrometry using dry, wet, and microwave ashing methods", *Atomic Spectroscopy*, *29*(3), 99-106, 2008.

[23] Sieber, R., Rehberger, B., Schaller, F., Gallmann, P., "Technological aspects of copper in milk products and health implications of copper", *ALP Science,* 493, 1-15, 2006.

[24] Yüzbaşı, N., Sezgin, E., "Süt ve ürünlerindeki bazı metal kontaminasyonlarının toksikolojik etkileri", *Gıda, (2)*, 121-122, 2002.

[25] Gördes Baş, H. Tüketime Sunulan Yoğurt Ve Buttermilklarda Ağır Metal Varlığının Araştırılması, Master's thesis, Afyon Kocatepe Üniversitesi, Afyon, Türkiye, 2020.

[26] Fahriye, K.A.N., Küçükkurt, İ., "Afyon manda kaymağı ve kaymakaltı sütlerinde bazı ağır metallerin ICP-MS ile araştırılması" *Kocatepe Veteriner Dergisi*, *11*(4), 447-453, 2018.

[27] Vahčić, N., Hruškar, M., Marković, K., Banović, M., Barić, I.C., "Essential minerals in milk and their daily intake through milk consumption", *Mljekarstvo/Dairy*, *60*(2), 77-85, 2010.

[28] Ayar, A., Sert, D., Akın, N., " Konya'da tüketime sunulan süt ve süt ürünlerinin ağır metal içeriklerinin belirlenmesi", *Selcuk Journal of Agriculture and Food Sciences*, 21 (41), 58 – 64, 2007.

[29] Türk Gıda Kodeksi: Gıda Maddelerindeki Bulaşanların Maksimum Yönetmeliği Hakkında Tebliğ. Tebliğ No: 2011- 28157, Ankara: Tarım ve Köy İşleri Bakanlığı, 2011.

[30] FAO/WHO- Food and Agriculture Organization/World Health Organization. Joint FAO/WHO food standards program: Codex committee on contaminants in foods (Editorial amendments to the general standard for contaminants and toxins in food and feed), sixth session, Maastricht, Netherlands, 26-30 march, 2012; CX/CF 12.6.11

[31] Hernandez, K., Park, Y.W., "Evaluation of 20 macro and trace mineral concentrations in commercial goat milk yogurt and its cow milk counterpart", *Food and Nutrition Sciences*, 5, 889-895, 2014.

[32] Conı, E., Bocca, B., Carolı, S., " Minor and trace element content of two typical Italian sheep dairy products", *Journal of dairy research*, *66*(4), 589-598, 1999.

Middle East Journal of Science

Research Article

PROTECTIVE BEHAVIOR AGAINST CORROSION OF POLY(N-METHYLANILINE) COATINGS ELECTROSYNTHESIZED ON STAINLESS STEEL SURFACE FROM SULFURIC ACID CONTAINING MONOMER SOLUTION*

Zeynel Doğruyol[1] *Aziz Yağan[2]*
[1]D. H. M. İ. Mardin Airport, Turkey
[2]Dicle University, Faculty of Education, Turkey
Corresponding author: zeyneldogruyol@gmail.com

Abstract: *Thanks to their outstanding optical and electrical properties, potential polymers are one of the materials with the highest potential use in technological applications. In this study Poly(N-methylaniline) coated stainless steel disc electrodes were obtained with N-methylaniline containing sulfuric acid solutions using constant potential, constant current and potentiodynamic techniques by electrodeposition. Corrosion behavior of polymer coated electrodes were investigated by direct current (DC) polarization technique and linear anodic cyclic voltammetry in different aqueous (NaCl and HCl) solutions. Electrochemical techniques branching test results showed that the electroactive PNMA coating can be used as a protective coating against rust for stainless steel. It was demonstrated that N-methylaniline aniline and pyrrole with an aqueous solution of H_2SO_4 as the electrolyte can also show positive copolymers and various coatings.*

Keywords*: Electropolymerization, Poly(N-methylaniline), Corrosion, DC polarization.*

1. Introduction

Corrosion has become one of the most serious problems of our day due to its economic, safety, and environmental effects. If protective coatings are used on metals or alloys exposed to corrosion, the world economy can be saved from the serious effects of corrosion losses. The use of protective coatings will reduce problems caused by corrosion and greatly increase the effective life of most metal-containing machines.

As a result of the studies, it has been determined that electroactive conductive polymers can be used as protective coatings since traditional methods used in protecting metals with oxidizing properties against corrosion can cause serious environmental problems. In particular, the electrodeposition of conductive polymers to common metals (Zn, Fe, Al) on the surface has been an important subject of study in recent years (Deberry 1985).

Conductive polymers not only act as a protective coating on metals in a corrosive environment but also prevent corrosive ions from reaching the metal surface due to their electroactivity when exposed to a corrosive environment for a long time (Sazou 1997). During electropolymerization, a more stable

passive oxide layer occurs at the electrode surface polymer interface compared to those obtained in the electrolysis solution containing the electrolyte with the monomer (Su 2000). For this purpose, conductive polymers such as PANI-Fe_2O_3 (Sumi 2020), polypyrrole (Ppy) (Mortazavi), PTh (Ai 2014), polyindol (Paved 2013) have been investigated due to their high environmental stability, non-toxic properties, and easily adjustable conductive oxidation state, simple and economical production methods.

In the study achieved by Döşlü et al., the protection efficiency of polyindole film on stainless steel was increased with titanium dioxide pre-coating. Characterization of the coatings was provided by nuclear magnetic resonance and Fourier transform infrared spectra. The surface morphology of electrodes was monitored by scanning electron microscopy. Corrosion performance was examined in %3.5 NaCl solution by electrochemical impedance spectroscopy and potentiodynamic measurements. Quantum calculations were made and theoretical parameters were determined. The results showed that there is a relationship between experimental and theoretical parameters. High protection efficiency against corrosion was observed on the steel surface by forming a protective polyindole top-coated titanium dioxide film (Döşlü et al 2013).

The PANI-Fe_2O_3 composite synthesized in the study by Sumi et al. was incorporated into a commercial alkyd resin and an effective anticorrosive coating for mild steel was developed. Both composite and fabricated alkyd resin coatings have been systematically characterized using FTIR, XRD, SEM, TEM, XPS, TGA, OSP, SKPM, and EDS. Corrosion-resistant properties of nanocomposite coatings were evaluated by potentiodynamic polarization, impedance spectroscopy, and long-term open circuit potential measurements at %3.5 NaCl and 1 M HCl. The much-improved corrosion resistance of the coating containing PANI-Fe2O3 has been associated with better barrier performance and passivation protection offered. The higher corrosion resistance observed in an acidic environment was explained by the complementary cathodic reaction of conductive emeraldin-PANI to non-conductive leuko-PANI. The manufacturing method provided may be useful for the development of environmentally friendly anti-corrosion "conductive polymer-metal oxide-alkyd resin" coatings (Sumi et al 2020).

In the study achieved by Mortazavi et al, polyethylene glycol (PEG) doped ammonium bifluoride doped Ppy and embedded Ppy coatings were deposited on AZ31 Mg alloy using cyclic voltammetry. The results of fluoride-nuclear magnetic resonance (F-NMR), thermal gravimetric analysis (TGA), and differential scanning calorimetry (DSC) showed that the fluoride additive in the polyethylene glycol molecule was applied. Corrosion performance of doped Ppy coatings was evaluated by electrochemical impedance spectroscopy (EIS) and potentiodynamic polarization techniques in 0.05 M NaCl solution. Field emission scanning electron microscopy (FESEM) and energy-dispersive x-ray spectroscopy (EDS) showed that doped Ppy coatings have higher corrosion resistance than Ppy coating. The load transfer resistance of the doped Ppy coating was measured approximately 2 and 5 times higher than the undoped Ppy and Ppy coatings, respectively, which is associated with the synergistic behavior of fluoride with polyethylene glycol as well as its release into the anodic regions.

In the study conducted by Ai et al., A simple, no template method was successfully implemented to prepare polythiophene microspheres with uniform size and well spherical shape using anhydrous $FeCl_2$ as catalyst and H_2O_2 as oxidant by one-pot chemical oxidation polymerization. The structure and morphology of polythiophene nanoparticles have been characterized by IR, SEM, and TEM. Polythiophene nanostructures exhibited good microsphere morphology with a very narrow particle size distribution. By fine-tuning the reaction conditions, polythiophene in different sizes and nanostructures can be obtained. The corrosion protection property of coatings containing polythiophene microsphere

on soft steel was investigated by electrochemical impedance spectroscopy (EIS) technique in % 3.5 NaCl aqueous solution by weight. The results showed that coatings containing water-based polythiophene microspheres (PTh content, % 0.6 by weight) can provide high protection because impedance values remained higher than $1 \times 106 \ \Omega \ cm^2$ after 360 hours. All results are comparable to pure water-based epoxy coatings on mild steel (Ai et al 2014).

PPy deposits were successfully electropolymerized potentiodynamically on a pre-passivated Fe electrode in an aqueous solution containing monomer and oxalic acid. Electropolymerization of PPy was carried out between 0.3 V and 0.8 V versus SCE with a scanning rate of 20 mV / s. Electrochemical properties of PPy coated Fe electrode was determined using cyclic voltammetry, galvanostatic charge-discharge cycle, and electrochemical impedance spectroscopy. The maximum specific capacitance of PPy coated Fe electrode is 2280 F/g. This demonstrates the applicability of the PPy coated Fe electrode. However, the PPy coated Fe system behaved like PAni and showed high capacitance, not like Ppy. Using the cyclic voltammetry technique from aqueous oxalic, 0.2 V and 1.1 V acid electrolyte solution were obtained against SCE with a scanning speed of 20 mV / s. The properties of adhesive and electroactive PNMA coatings have been successfully investigated using the cyclic voltammetry technique. On the other hand, electrochemical impedance spectroscopy (EIS) was used to examine the long-term corrosion performance of PANI and PNMA coated electrodes separately in 0.5 M NaCl and 0.5 M HCl solutions. EIS measurement results showed that PANI and PNMA coatings improve protection for SS in neutral and acidic corrosive solutions. In addition, PANI and PNMA coatings were able to offer protection to SS electrodes for a longer immersion time in NaCl solution compared to HCl. After immersion in NaCl for 168 hours, the PANI coating of the steel was insufficient to prevent corrosion, while the PNMA coating lost its protective properties after 240 hours (Yagan 2019).

In the study conducted by Yagan et al., Poly (N-ethylaniline) (PNEA) coatings were deposited on Fe and Pt-disk electrodes by potentiodynamic synthesis technique. The coating was carried out using an aqueous solution of oxalic acid containing the monomer of N-ethylaniline. PNEA polymer growth was found to be much less than on the Pt surface. On the surface of Fe. PNEA coatings have been characterized both electrochemically and spectroscopically. Linear anodic potentiodynamic polarization, Tafel test, and electrochemical impedance spectroscopy techniques were used in the corrosion protection coating 0.5 M H_2SO_4, 0.1 M HCl, and 0.5 M NaCl solutions of PNEA. For comparison, PANI was also used on the Fe surface by potentiodynamic synthesis technique. The presence of PNEA and PANI coatings on the Fe electrode limits the dissolution potential range with respect to the linear anode. Potentiodynamic polarization curves obtained in 0.5 M H_2SO_4, the maximum dissolution current density values for PNEA and PANI coated Fe electrodes were 10.7 mA cm2 and 11.6 mA cm^2, respectively. These current density values were found to be significantly lower compared to bare. electrode (41.8 mA cm^2). Tafel test results have shown that the PNEA coating exhibits significant corrosion protection properties in the NaCl environment. That of the HCl medium. Long-term impedance measurements of PNEA coated and uncoated electrodes in NaCl and HCl solutions, corrosion protection properties of PNEA coating in NaCl environment (135.02 $\Omega \ cm^2 \ R_{ct}$ value after 196 hours) compared to significantly higher HCl environment (20.30 $\Omega \ cm^2 \ R_{ct}$ value after 48 hours) It has been determined that the corrosion results obtained independently, electrochemical methods in three different corrosive environments are in full harmony with each other (Yagan et al 2007).

In this study, we investigated the effect of PNMA on stainless steel electrodes in aqueous sulfuric acid solutions of electrosynthesis conditions. The conductivity of polymer layers against corrosion on

the alloyed surfaces was examined and compared in sulfuric acid solutions, linear potentiodynamic polarization, DC polarization test technique, and NaCl, HCl, and H_2SO_4 solutions.

2. Methods

Electrochemically prepared coatings were immersed in distilled water to remove the adsorbed electrolyte monomer and soluble oligomers formed during the electroplating process of the coating and then dried at room temperature.

2.1. Linear anodic potentiodynamic polarization method

Anti-corrosion control of polymer-coated and uncoated electrodes was performed in 0.5 M H_2SO_4 aqueous solutions at 10 mv / s with 1 \ 2 cycles with potentiodynamic scanning method in the potential region between -0.3 V and +0.9 V and SCE.

2.2. DC Polarization

It is a potentiodynamic corrosion test method. DC polarization tests were performed under continuously mixed conditions with a capillary bridge containing a thin terminal block to minimize ohmic resistance. Anodic and cathodic polarization curves were recorded by varying the electrode potential between -650 mV + 250 mV with a constant sweep rate of 1 mV / s in an unventilated 0.5 M NaCl, 0.5 M HCl.

3. Results

The behavior of uncoated and PNMA coated electrodes when a 0.5 V vs SCE constant potential is applied in a corrosive 0.5 M HCl solution is given in Figure 1. The solid line curve shows that stainless steel dissolves strongly at this potential. When the same electrode is coated with PNMA by electrosynthesis and this surface is exposed to a constant potential of 0.5 V, it is seen that the behavior changes completely. First of all, there is no dissolution observed in the uncoated electrode. This indicates that the layer on the surface protects the stainless steel surface. This experiment result given a strong indication that the PNMA coating can provide effective protection against corrosion.
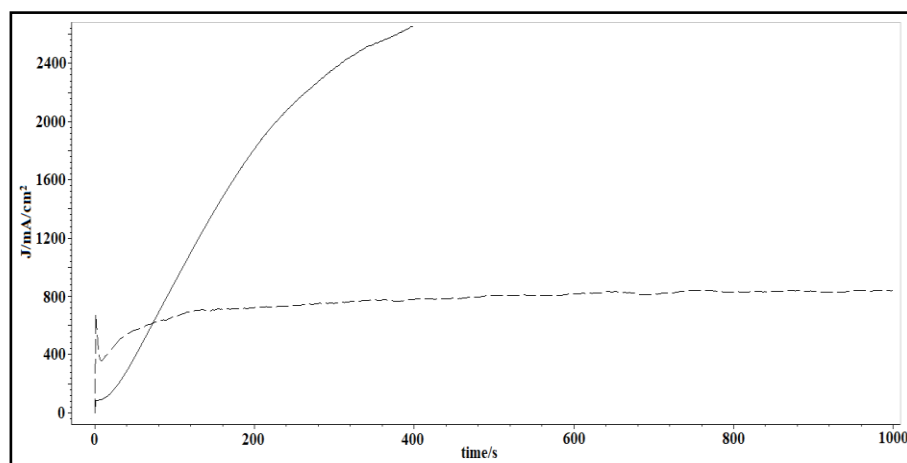

Figure 1. The behavior of the polymer when a 0.5 V constant potential is applied to the uncoated and PNMA coated electrodes in a corrosive 0.5 M HCl solution.

Figure 2. shows the behavior of the polymer when a 0.5 V constant potential is applied to the uncoated and PNMA coated electrodes in a corrosive 0.5 M NaCl solution. The solid line curve shows that stainless steel dissolves strongly at this potential. When the same electrode is coated with PNMA with electrosynthesis and this surface is exposed to a constant potential of 0.5 V, it is seen that the behavior changes completely. First of all, there is no dissolution observed in the uncoated electrode. This indicates that the layer on the surface protects the stainless steel surface. This experiment gives a strong indication that the PNMA coating can provide effective protection against corrosion.
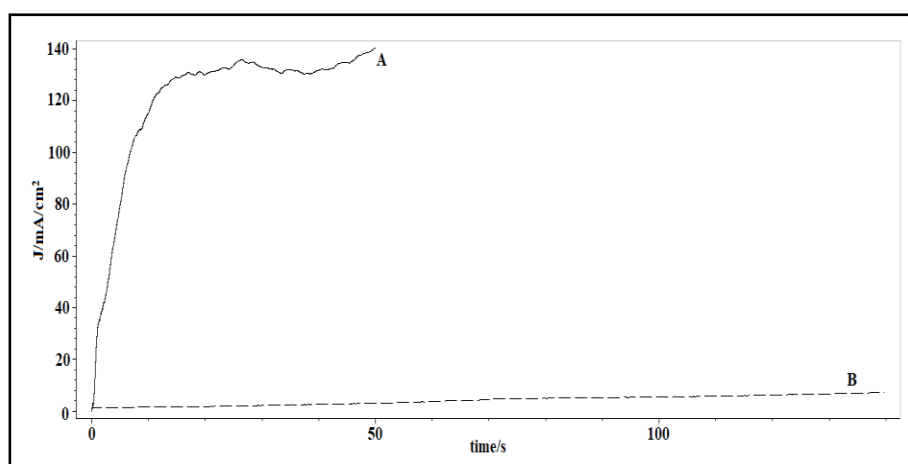

Figure 2. The behavior of the polymer when a 0.5 V constant potential is applied to the uncoated and PNMA coated electrodes in a corrosive 0.5 M NaCl solution.

Figure 3 shows the Tafel curves obtained in 0.5 M NaCl solution of uncoated PNMA coated electrodes obtained at 10 mv/s scanning speed. The increasing of the coated electrode to the positive potential and the decrease in the current values, especially on the anodic side, are indicators of the protection of the coating
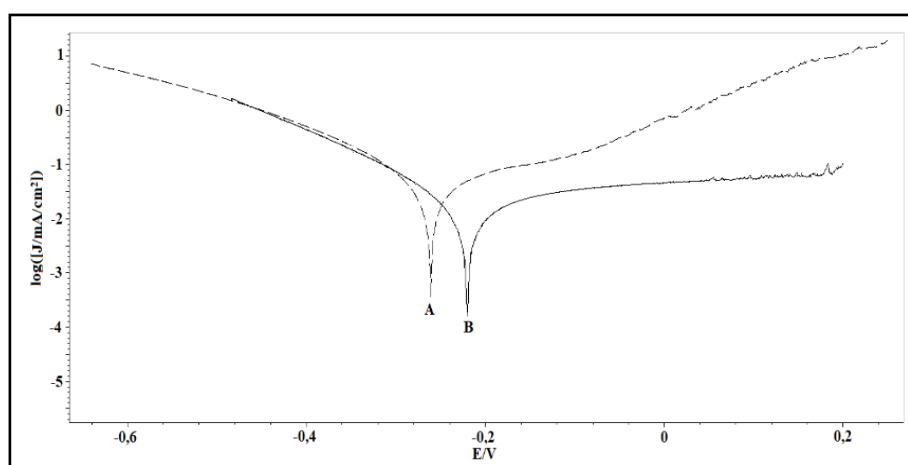

Figure 3.Tafel curves obtained in 0.5 M NaCl solution of PNMA coated electrodes with uncoated and 10 mv / s scanning speed (A: Uncoated; B: Coated)

Figure 4 shows the Tafel curves obtained in 0.5 M HCl solution of PNMA coated electrodes obtained at a scanning speed of 10 mv/s and uncoated. The attraction of the coated electrode to the positive potential and the decrease in the current values, especially on the anodic side, are indicators of the protection of the coating. When the behavior of coated electrodes in B and C curves is compared against uncoated electrodes, it is clear that PNMA coating protects better in HCl than NaCl; The corrosion current exhibited by the coated electrode has shifted considerably to noble potentials.
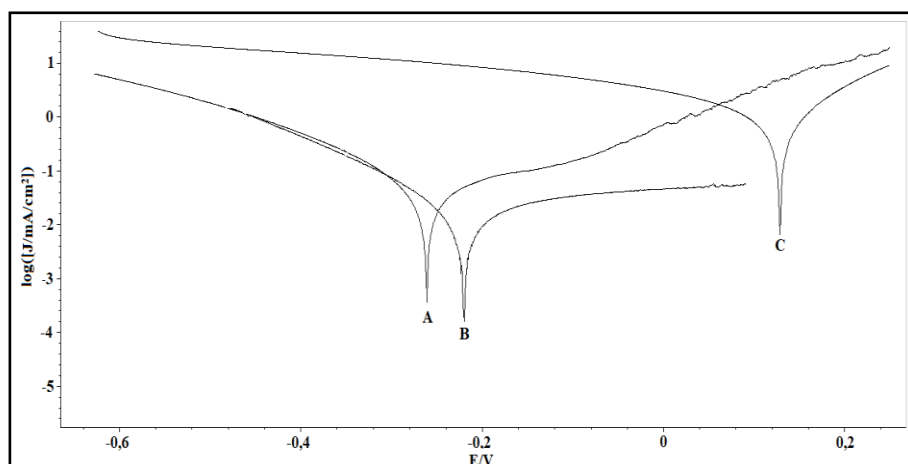
Figure 4. Tafel curves obtained in 0.5 M HCl and 0.5 M NaCl solution of PNMA coated electrodes obtained at 10 mv/s scanning speed without coating (C: HCl environment)

4. Discussion

The characterization process for PNMA coated steel electrodes was carried out by electrochemical technique and the polymer was obtained. The extent to which the PNMA coated electrode surfaces obtained protects the steel against corrosion was determined by linear chronoamperometry, potentiodynamic polarization, and the Tafel method. According to corrosion test results, the stainless steel of the electroactive PNMA coating can be used as corrosion protection and coating.

The electrolyte can be an aqueous H_2SO_4 solution. N-methylaniline copolymers with aniline and pyrrole, and various coatings.

The compliance to the Research and Publication Ethics: This study was carried out in accordance with the rules of research and publication ethics.

References

[1] Ai, L., Liu, L., Zhang, X., Ouyang, X., Ge, Z., '' A facile and template-free method for preparation of polythiophene microspheres and their dispersion for waterborne corrosion protection coatings'' *Synthetic metals* Vol (191), pp.41- 46, 2014.

[2] Döşlü, S., Mert, B., Yazıcı, B., ''Polyindole top coat on TiO_2 sol–gel films for corrosion protection of steel'' *Corrosion science* Vol (66), pp.51-58, 2013.

[3] Deberry, W., *J. Electrochemical Society.* Vol (132), pp.1022, 1985.

[4] Mortazavi, S., Yeganeh, M., Etamed, A., Saremi, M., '' Corrosion behavior of polypyrrole (Ppy) coating modified by polyethylene glycol (PEG) doped ammonium bifluoride on AZ31 magnesium alloy'' *Progress in Organic Coatings* Vol (134), pp.22-32, 2019.

[5] Sazou, D., Georgolios, C., '' Formation of conducting polyaniline coatings on iron surfaces by electropolymerization of aniline in aqueous solutions'' *Journal of Electroanalytical Chemistry* Vol (429) pp.81-93, 1997.

[6] Sumi, V., Arunima, S., Deepa, M., Sha, M., Riyas, A., Meera, M., Saji, V., Shibli, S., '' PANI-Fe_2O_3 composite for enhancement of active life of alkyd resin coating for corrosion protection of steel'' *Materials Chemistry and Physics* Vol (247), pp.122881, 2020.

[7] Yağan, A., Pekmez, N., Yıldız, A.,'' Investigation of protective effect of poly(N-ethylaniline) coatings on iron in various corrosive solutions'' *Surface & Coatings Technology* Vol (201) pp.7339-7345, 2007.

[8] Yağan, A., '' Investigation of Polypyrrole-Based Iron Electrodes as Supercapacitors'' *International Journal of electrochemical science* Vol (14), pp. 3978-3985, 2019.